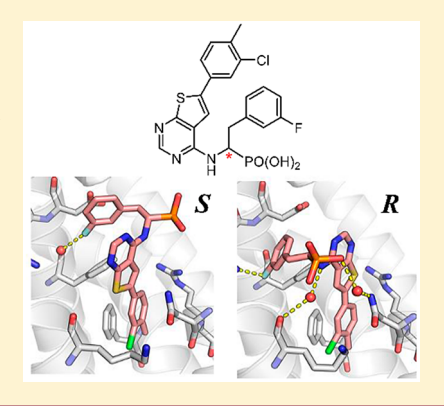


Chirality-Driven Mode of Binding of α -Aminophosphonic Acid-Based Allosteric Inhibitors of the Human Farnesyl Pyrophosphate Synthase (hFPPS)

Yuting Feng,[†] Jaeok Park,^{†,‡} Shi-Guang Li,[†] Rebecca Boutin,[†] Peter Viereck,[†] Matthew A. Schilling,[‡] Albert M. Berghuis,*^{*,‡} and Youla S. Tsantrizos*^{*,†,‡}

Supporting Information

ABSTRACT: Thienopyrimidine-based allosteric inhibitors of the human farnesyl pyrophosphate synthase (hFPPS), characterized by a chiral α -aminophosphonic acid moiety, were synthesized as enantiomerically enriched pairs, and their binding mode was investigated by X-ray crystallography. A general consensus in the binding orientation of all (R)- and (S)-enantiomers was revealed. This finding is a prerequisite for establishing a reliable structure-activity relationship (SAR) model.



■ INTRODUCTION

Human farnesyl pyrophosphate synthase (hFPPS) is the gatekeeper of mammalian isoprenoid biosynthesis and a validated therapeutic target for bone-related diseases. The catalytic product of hFPPS is the C-15 isoprenoid farnesyl pyrophosphate (FPP), which is formed from the successive condensation of two C-5 isopentenyl pyrophosphate (IPP) units with dimethyl allyl pyrophosphate (DMAPP). FPP is a key precursor to many essential metabolites, including geranylgeranyl pyrophosphate (GGPP). Blocking post-translational farnesylation or geranylgeranylation of small GTPbinding proteins (GTPases), particularly members of the RAS superfamily that are known drivers of oncogenesis, has been proposed as a potential novel mechanism for treating cancer.² However, bona fide and clinically validated antitumor agents that selectively target hFPPS have not yet been identified. Currently, nitrogen-containing bisphosphonates (N-BPs; e.g., zoledronic acid 1) are the only approved drugs that selectively target hFPPS. These inhibitors bind to the allylic subpocket of the active site and exhibit low nanomolar intrinsic potency (e.g., the IC₅₀ value of the most potent known inhibitor 1 is ~2-4 nM).3 It has been assumed that the highly charged nature of the bisphosphonate pharmacophore of N-BPs, which exists as the trianion under physiological conditions, limits their cell membrane permeability, systemic circulation, and exposure to nonskeletal tissues. Nonetheless, clinical data obtained from patients treated with 1, in addition to standard chemotherapy, suggest that this compound may have some therapeutic value in the treatment of cancers such as multiple

myeloma⁴ and breast cancer.⁵ Consequently, the identification of more "drug-like" (in the classical sense) inhibitors of hFPPS has attracted significant attention in recent years.

The discovery of a catalytically relevant, allosteric pocket near the IPP binding subpocket of the active site⁶ has fueled interest in the discovery of nonbisphosphonate inhibitors that can bind to this pocket and may exhibit superior biopharmaceutical properties than those of N-BPs. This allosteric pocket was found to play a critical role in the feedback mechanism of the enzyme, which is Nature's way of controlling the intracellular concentrations of FPP. To date, many nonbisphosphonate, allosteric inhibitors of hFPPS have been reported; some examples are shown in Figure 1.8

In the course of our own investigations, we discovered a new chemotype of allosteric inhibitors, the C6-substituted thienopyrimidine-based monophosphonate (C⁶-ThP-MP) analogues 6 (Figure 1). These analogues are characterized by a chiral α -aminophosphonic acid moiety, which was previously shown to adopt two different binding orientations. A general consensus in the binding mode of all analogues within a structural class of inhibitors is a prerequisite for establishing a reliable structure-activity relationship (SAR) model. A predictive SAR model is the hallmark of medicinal chemistry and drug discovery. Therefore, we embarked on an investigation into the role of the α -aminophosphonic acid in controlling the binding orientation of this class of inhibitors. In

Received: July 9, 2019 Published: October 2, 2019

[†]Department of Chemistry, McGill University, 801 Sherbrooke Street West, Montreal, Quebec H3A 0B8, Canada

[‡]Department of Biochemistry, McGill University, 3649 Promenade Sir William Osler, Montreal, Quebeck H3G 0B1, Canada

Figure 1. Examples of active site (1) and allosteric inhibitors (2-7) of hFPPS.

this report, we describe the synthesis of several enantiomeric pairs of 6 and demonstrate that their chirality controls the binding orientation and interactions of these inhibitors with the hFPPS allosteric pocket.

■ RESULTS AND DISCUSSION

The asymmetric synthesis of α -aminophosphonic acids is of considerable interest in drug discovery. These bioisosteres of amino acids are useful building blocks in the design of potential therapeutic agents, including HCV protease inhibitors. A number of methodologies for their asymmetric synthesis have been previously reported. Recent examples include metal-catalyzed asymmetric hydrogenation of α , β -dehydroaminophosphonates, α -iminophosphonates, and α -hydrazono phosphates, asymmetric hydrophosphonylation of imines, α [3 + 2] cycloaddition of dehydroaminophosphonates and α -tosylhydrazones, and other enantioselective C–C bond forming reactions that can lead to the formation of chiral quaternary α centers, as well as the asymmetric three component Kabachnik–Fields condensations.

In this study, we adopted the asymmetric 1,4-addition of aryltrifluoroborates to dehydroaminophosphonate catalyzed by a Rh-Difluorphos complex for the preparation of the (R)- α -

aminophosphonates with a benzylic side chain as previously reported by Darses (Scheme 1, path A). 18 Preparation of various (R)-acetamido phosphonate esters 10 was initiated with the preparation of diethyl (1-acetamidovinyl)phosphonate 8, following the protocol previously reported. 18 The subsequent 1,4-addition of various aryltrifluoroborates or boronic acids (9) to 8 proceeded to give the desired products (R)-10 in 70-75% isolated yields and 85-90% enantiomeric excess (Scheme 1, path A). Because the (R)-Difluorphos ligand is not commercially available, we decided to screen several other commonly used phosphorus-based ligands (e.g., BINAP, SEGPHOS, and many others) for the preparation of intermediates (S)-10. However, all of the ligands tested led to significantly lower enantiomeric purity of the (S)-10 products. For example, only 55% ee was observed with both (S)-BINAP and (S)-SEGPHOS in the synthesis of analogue (S)-10a. Recently, a site-selective and enantioselective modification of an amino acid moiety in the natural product thiostrepton was reported by Key and Miller. 19 In this transformation, 1,4-addition of an arylboronic acids to an olefinic moiety was catalyzed by [Rh(nbd)₂]BF₄ in the presence of (S,S)-Chiraphos as the ligand. We adopted this method and successfully synthesized various (S)-10 building

Scheme 1. Asymmetric Synthesis of α -Aminophosphonic Acid hFPPS Allosteric Inhibitors^a

"Reagents and conditions: (a) $[Rh(C_2H_4)_2Cl]_2$ (1.5 mol %), (S)-Difluorphos (3.3 mol %), NaHCO₃ (2 equiv), iPrOH, 90°C, 18 h (70–80% yield); (b) Rh(nbd)₂BF₄ (7.5 mol %), (S,S)-Chiraphos (8 mol %), Na₂CO₃ (1 equiv), MeOH (8 equiv), dioxane/H₂O, 70°C, 20 h (60–70% yield); (c) (i) Boc₂O, DMAP (cat.), THF, 80°C, 4 h, (ii) LiOH·H₂O, THF/H₂O (2:1), RT, 20 h, (iii) HCl (4M in dioxane), DCM, RT, 3 h (50%); (d) Et₃N, DMSO, 100°C, 2 h (50–80%); (e) TMSBr/MeOH, RT, 24 h (40–80% yield); (f) HPO(OEt)₂, (R,R)- or (S,S)-ProPhenol/Et₂Zn (10 mol %) toluene, 0 °C, 0.5 h (30% yield); (g) $[Rh(cod)_2]BF_4$ (3 mol %), (S)-BINAP (6 mol %), guaiacol (1 equiv), toluene, 110 °C, 16 h (50% yield).

blocks in good yield (\sim 70%) and enantiomeric purity (70–80% ee; Scheme 1, path B).

Unfortunately, neither of the above methods (i.e., paths A or B) were successful in the preparation of analogues 10 with an alkyl side chain (e.g., cyclohexyl derivative 10c; Scheme 1, path C). Such analogues were prepared by asymmetric phosphorylation of the N-acylimine intermediate 11 catalyzed by diethyl zinc in the presence of Trost's (S,S)- or (R,R)- ProPhenol ligands,²⁰ as previously reported by Wang.²¹ Although both the (R)- and (S)-10c were obtained in high enantiomeric purity (\sim 95% ee), the isolated yields were low (\sim 30%). Isomerization of imine 11 to the corresponding enamide 12 was observed as the main side product and the likely reason for the low yields. This isomerization has been previously observed with other similar systems²² and suggests that this methodology (i.e., Scheme 1, path C) would likely be even more problematic for the preparation of benzylic analogues, such as 10a and 10b.

The subsequent removal of the *N*-acyl or *N*-benzoyl protecting groups of all intermediates **10** was achieved under mild conditions using a 3-step protocol, which involves the amide-to-carbamate transformation originally reported by Burk and Allen. ²³ The Boc group was cleaved under standard acidic

conditions to liberate the free amine intermediates 13 (Scheme 1). Nucleophilic addition of amines 13 to the 4-fluoro-6-(p-tolyl)thieno[2,3-d]pyrimidine scaffold 14a,b via S_N Ar, followed by deprotection of the phosphonate ethyl esters, as previously reported, 9 gave the final C^6 -ThP-MP inhibitors (R)- and (S)-6d-6h (Figure 1).

To probe the binding contributions of the phosphonate group, we also synthesized the α -amino acid derivative of our most potent inhibitor **6g**. The synthesis of the amino acid (S)-17 was achieved starting with 1,4-addition of aryltrifluor-oborate **9d** to commercially available methyl 2-acetamidoacrylate (Scheme 1), followed by deprotection of both the amine and the carboxylic acid moieties using the same protocol as for the conversion of the α -aminophosphonates **10–13**. For the synthesis of (R)-17, the best enantiomeric purity was achieved using the rhodium-catalyzed 1,4-addition of **9d** in the presence of (S)-BINAP and guaiacol, as previously reported by Darses.²⁴

Previously, in an effort to expedite optimization of our initial hit compound **6a** and establish SAR, a library of C⁶—ThP-MP analogues was prepared in racemic mixtures (Figure 1). In this approach, a presumption was made that the potency observed with the racemic compounds would be mainly due to one enantiomer. In addition, it was assumed that the potent

(or more potent) enantiomer was more likely to bind and cocrystallize with the enzyme. However, when enantiomerically enriched inhibitors (R)- and (S)-6 were prepared, to our surprise, only a 2-3-fold difference in potency was observed, suggesting that more than one binding mode was possible for this class of compounds. This assumption was confirmed by the cocrystal structures of several analogues, including those of inhibitors 6a, 6b, and 6g, which bound to the hFPPS allosteric pocket in two distinct orientations (Figure 2; cocrystallizations

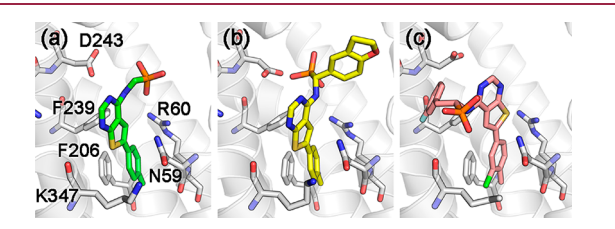


Figure 2. Previously determined cocrystal structures of C^6 -ThP-MP inhibitors **6** (racemic samples of inhibitors **6b** and **6g** were used): (a) **6a**, (b) **6b**, and (c) **6g** bound in the allosteric pocket of hFPPS. For clarity, protein residues are only labeled in (a).

were carried out with the racemic mixtures of the inhibitors).9 Interestingly, the aromatic 6-tolyl thienopyrimidine core was the only part of these molecules that adopted consistent binding interactions with the protein, engaging in an edge-toface π -stacking interaction with the side chain of Phe239 and a sandwich of π -stacking interactions with the side chains of Phe206 and Asn59. In contrast, the entire molecule 6g was flipped by approximately 180° as compared to 6a and 6b, and consequently, the α -aminophosphonate moiety of each compound adopted a completely different orientation (Figure 2). For example, in analogue 6a, the phosphonate moiety was bound facing the active site and close to the guanidinium ion of Arg60 (from here on referred to as the "up orientation"; Figure 2a), whereas in analogue 6g, the phosphonate was bound nearly in the opposite direction and toward the solventexposed surface of the cavity (from here on referred to as the "down orientation"; Figure 2c).

In this study, we reinvestigated the molecular interactions between hFPPS and several pairs of (R)- and (S)-enantiomers of the C⁶-ThP-MP inhibitors (6) by X-ray crystallography. A general consensus in the binding orientation for all (S)-6/ enzyme complexes (Figure 3a,c,e) and a different consensus in binding for all the (R)-6/enzyme complexes (Figure 3b,d,f) were observed. Regardless of the presence of a substituent on the C-6 tolyl moiety attached to the thienopyrimidine core and/or a substituent on the $C\alpha$ benzyl moiety of the α aminophosphonate moiety (i.e., R1), all of the inhibitors with the (S)-stereochemistry were found to bind with the phosphonate in the "up-orientation" (Figure 3a,c,e), whereas all the (R)-enantiomers bound with the phosphonate in the "down-orientation" (Figure 3b,d,f). It should be noted that all crystals were obtained under slightly basic conditions (i.e., pH $\sim 7.5-8.5$) to ensure (inasmuch as it is possible) that the phosphonate moiety of the enzyme-bound inhibitors were fully deprotonated; reported p K_a s of α -aminophosphonates are in the range of 2.3 (1st p K_a) to 6.0 (2nd p K_a). It is noteworthy that inhibitor (R)-6b, which has a larger aromatic substituent directly attached to the $C\alpha$ carbon, displays a different binding orientation (Figure 2b). As we previously reported,9 this is likely due to anticipated steric clashes between the dihydrobenzofuran moiety and residues of the $\alpha_{\rm H}$ and $\alpha_{\rm I}$

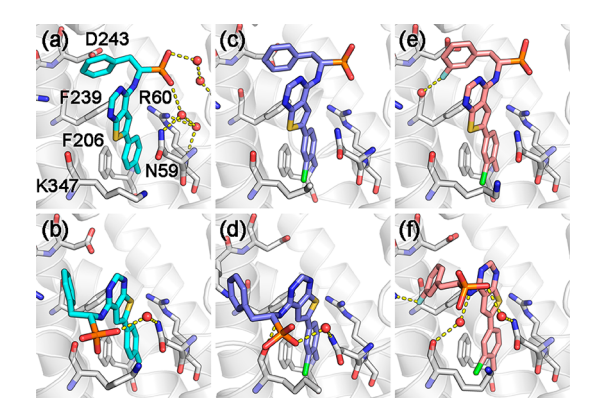


Figure 3. Cocrystal structures of inhibitor/hFPPS complexes. Inhibitors: (a) (*S*)-6d (PDB 6N7Z), (b) (*R*)-6d (PDB 6N7Y), (c) (*S*)-6f (PDB 6OAG), (d) (*R*)-6f (PDB 6OAH), (e) (*S*)-6g (PDB 6N82), and (f) (*R*)-6g (PDB 6N83). The red spheres represent water molecules.

helices of the protein, which prevent this compound from binding in the "down orientation". Such unfavorable interactions may also induce an unusual microenvironment protonation of the D243 carboxylate side chain, which is found to bind close to the phosphonate moiety of the inhibitor. However, because inhibitors with an aromatic moiety directly attached to the $C\alpha$ carbon are less potent that the benzylic analogues, we did not explore these analogues any further.

We further examined the effects of the 3-chloro substituent on the C-6 tolyl moiety, which was previously found to improve the in vitro potency of these compounds. The cocrystal structures of inhibitors (R)-6f and (R)-6g (parts d and f of Figure 3, respectively), which bind in the "down orientation", revealed that the 3-chloro moiety contributed to the binding affinity of these inhibitors by making the entire tolyl side chain occupy the allosteric pocket more tightly (Figure 4b,c vs a). Additionally, the binding of the chlorine

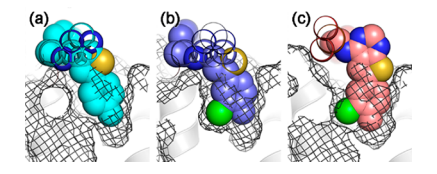


Figure 4. Sideview of (R)-enantiomeric C^6 -ThP-MP inhibitor binding in space-filling representation. (a) (R)-6d, (b) (R)-6f, and (c) (R)-6g.

substituent induced some movement to the scaffold, which led to either a direct (Figure 3d) or a water-mediated H-bond between the exocyclic C-4 nitrogen of the thienopyrimidine core and the carbonyl oxygen of Lys347 (Figure 3f). In contrast, with inhibitors (S)-6f and (S)-6g (parts c and e of Figure 3, respectively), which bind in the "up orientation", the 3-chloro moiety pushed the scaffold upward by \sim 1 Å, causing the loss of several water-mediated interactions between the phosphonate moiety and the protein (e.g., to Asn59 and Arg60; Figure 3a). These water-mediated interactions were previously observed with several analogues, including our initial hit, compound f (Figure 2a), and presumed to contribute to the binding affinity of these inhibitors.

Substitution on the $C\alpha$ benzyl (i.e., Figure 1; inhibitor 6, R^1) of the α -aminophosphonate also played a significant role in the inhibitor/enzyme complex formation. For example, the 3-

fluorobenzyl substituent in analogues 6e and 6g introduced additional binding interactions with the protein. The fluorine atom in (S)-6g formed water-mediated H-bonds with the carbonyl of Phe239 and Gln242 (Figure 3e), whereas in the (R)-enantiomer of 6g, the fluorobenzyl moiety packed more tightly against the protein surface engaging in stronger van der Waals interactions, and the benzyl ring made a stacking interaction with the side chain of Phe239 (Figure 3f). Additionally, the fluorine atom appeared to form a direct nonclassical H-bond with the NH amide of Gln242. These interactions pushed the thienopyrimidine scaffold significantly toward the active site while burying the 3-chlorotolyl group deeper into the allosteric pocket (Figure 4c) and contributed to the formation of the water-mediated H-bond between the exocyclic C-4 NH of the thienopyrimidine and the carbonyl oxygen of Lys347, mentioned above (Figure 3f). Although the position of the phosphonate group was also shifted, the interaction with the water molecule bound to Asn59 was retained (Figure 3f). Interestingly, all hFPPS inhibitors having the (R)-absolute stereochemistry and a 3-chloro substituent on the C-6 tolyl moiety were found to be more potent than their corresponding (S)-enantiomers in our in vitro hFPPS inhibition assay (Table 1). These results are consistent with the more extensive network of inhibitor/protein interactions observed by X-ray crystallography.

Table 1. Enzyme Inhibition (IC₅₀) of Representative Allosteric hFPPS Inhibitors^a

		2	
compd	hFPPS IC ₅₀ (μ M)	\mathbb{R}^2	% ee
2a	1.3 ^b		
6a	5.0	Н	
(S)-6d	2.8	Н	71 ^c
(R)-6d	7.7	Н	90 ^c
(S)- 6e	1.2	Н	86 ^c
(R)- 6e	2.8	H	80 ^c
(S)-6f	3.7	Cl	71^c
(R)-6f	1.5	Cl	92^c
(S)-6g	1.1	Cl	87^c
(R)-6g	0.54^{b}	Cl	78^c
(S)-6h	8.1	Cl	91°
(R)-6h	3.0	Cl	99 ^c
(S)-7 b	>10	Cl	83
(R)-7 b	1.0	Cl	80

 $^{a}\text{IC}_{50}$ values were determined with 10 min preincubation of the enzyme with each inhibitor; the values shown are average of $n \geq 3$ determinations with standard deviation of ± 5 –10%. Inhibitor 2a was used as the positive control in each assay. b Assays were run in parallel, average values of n = 6 determinations. c The enantiomeric purity (% ee) of analogues 6 was estimated from the chiral HPLC data of their precursor diethyl esters 15.

In our previous studies, we compared our initial hit, the α -aminophosphonate $\mathbf{6a}$, with the corresponding carboxylic acid derivative $\mathbf{7a}$ and found the latter to be significantly less potent (IC₅₀ values of 4.5 μ M and >20 μ M for compounds $\mathbf{6a}$ and $\mathbf{7a}$, respectively). Although the carboxylic acid analogue (R)-7b was found to be considerably more potent (IC₅₀ value of 1 μ M) than $\mathbf{7a}$, the (S)-7b was essentially inactive at the highest concentration test of 10 μ M (Table 1). Unfortunately, we were not able to obtain a cocrystal structure of (R)-7b bound to hFPPS. In the absence of direct structural evidence, we cautiously rationalize that binding of (R)-7b should corre-

spond to that of the phosphonate derivatives (S)-6g (i.e., binding in the "up orientation"), and because the phosphonate moiety of this analogue [i.e., (S)-6g] does not form any interactions with the protein, its replacement with a carboxylic acid should have negligible impact on potency. This hypothesis is consistent with the almost identical potency observed for the carboxylic acid analogue (R)-7b and the corresponding phosphonate derivative (S)-6g (Table 1; IC₅₀ values of 1.1 vs 1.0 μ M, respectively). By analogy, inhibitor (S)-7b would be expected to bind in the "down orientation" [analogous to (R)-6g], and the smaller electron density and size of the carboxylate moiety could lead to loss of the water-mediated H-bond that was previously observed between the phosphonate moiety and Asn59 (Figure 3f), leading to significant loss of potency. Currently, we cannot exclude the possibility that without the phosphonate group engaging in this interaction, the fluorobenzyl moiety may not be able to position itself correctly for optimal binding, leading to further loss in binding affinity [i.e., as seen with (R)-6g].

CONCLUSION

In summary, we synthesized a cluster of enantiomerically enriched pairs of $C\alpha$ -substituted aminophosphonate-based allosteric inhibitors 6 of the human FPPS and demonstrated that the binding mode of these compounds is driven primarily (if not exclusively) by their chirality. A general consensus in the binding mode of all (S)-enantiomers (Figure 3a,c,e) and all (R)-enantiomers (Figure 3b,d,f) was observed. These results can guide our future efforts in establishing a reliable SAR model. Independent optimization of the (R)- and (S)-enantiomers, expected to lead to divergent SAR, could also lead to more potent and selective allosteric inhibitors of hFPPS that can be used in vivo to confirm hFPPS as a validated biological target for oncology.

■ EXPERIMENTAL SECTION

General Information. All reactions were carried out under an atmosphere of dry argon unless otherwise specified. Completion of all reactions was monitored by TLC and/or LC-MS. Flash column chromatography was performed on silica gel (Sigma-Aldrich, 60 Å, 230-400 mesh, 40-63 μ m) as the stationary phase. Thin layer chromatography (TLC) was performed on alumina plates precoated with silica gel (MilliporeSigma, 60 Å, F254) and visualized by UV fluorescence when applicable ($\lambda_{max} = 254 \text{ nm}$) and/or by staining with Seebach's Magic Stain (acidic aqueous solution of polymolybdic acid and cerium(IV) sulfate), ninhydrin, or basic aqueous KMnO₄ solution. All compounds were fully characterized by ¹H, ¹³C, ¹⁹F, ³¹P NMR, and HRMS. ¹H NMR were recorded at 400 or 500 MHz, and coupling constants (J) are reported to ± 0.5 Hz. $^{13}C\{^1H\}$ NMR were recorded at 125 MHz and ³¹P{¹H} NMR were recorded at 202 MHz, unless otherwise indicated. Chemical shifts (δ) are reported in ppm relative to the internal deuterated solvent. Enantiomeric purity of chiral compounds was determined by chiral HPLC using an Agilent 1100 series instrument and the column type and solvent system indicated. Enantiomeric purity (% ee) was determined at two stages: intermediates 10 and 15 for the α -aminophosphonate analogues, as well as 16 and final compound 7b for the carboxylic acid inhibitor. The absolute stereochemistry of the major enantiomer in all new α aminophosphonates and α -amino acids were assigned by analogy with previously reported compounds in the literature. These assignments were further confirmed from the cocrystal structures of inhibitors (*R*)and (S)-6d, (R)- and (S)-6f, and (R)- and (S)-6g. The homogeneity of all final inhibitors, compounds (R)- and (S)-6d-6h and 7b were confirmed to >95% by ¹H NMR and C18 reversed phase HPLC, using an Atlantis T3 OBD, 5 μ m, 4.6 mm \times 100 mm column and a

linear gradient of H_2O :MeCN from 95:5 to 5:95 in 13 min then 100% MeCN for 2 min at a flow rate of 1 mL/min (all solvents contained 0.1% formic acid). LRMS were obtained on a Waters LC-MS instrument with ESI \pm modes. HRMS were obtained on a TOF instrument with ESI \pm modes, and the quoted masses are accurate to \pm 5 ppm. The names of the molecules that appear in the following pages were generated using ChemBioDraw Ultra 12.0.

General Procedure for the Preparation of Final Inhibitors 6. Synthesis of the thienopyrimidine scaffolds 14, the S_N Ar reaction between 13 and 14, as well as the final deprotection of the phosphonate esters 15, to obtain the phosphonic acid inhibitors 6 were previously reported.

(R)- or (S)-(2-Phenyl-1-((6-(p-tolyl)thieno[2,3-d]pyrimidin-4-yl)-amino)ethyl)phosphonic Acid [(R)- or (S)-6d]. Both compounds were isolated as off-white solids: (R)-6d, 3 mg, 37% yield; (S)-6d, 15 mg, 90% yield (yields indicated are for the last deprotection step). $^1\mathrm{H}$ NMR (500 MHz, $\mathrm{D_2O}$): δ 7.88 (s, 1H), 7.75 (s, 1H), 7.60 (d, J = 8.1 Hz, 2H), 7.34 (d, J = 7.2 Hz, 2H), 7.24 (d, J = 8.0 Hz, 2H), 7.13 (t, J = 7.4 Hz, 2H), 7.06 (t, J = 7.3 Hz, 1H), 4.59 (ddd, J = 15.2, 12.4, 3.0 Hz, 3H), 3.46 (d, J = 13.8 Hz, 1H), 2.92 (td, J = 13.1, 6.5 Hz, 1H), 2.37 (s, 3H). $^{31}\mathrm{P}\{^{1}\mathrm{H}\}\mathrm{NMR}$ (203 MHz, $\mathrm{D_2O}$): δ 15.84. $^{13}\mathrm{C}\{^{1}\mathrm{H}\}\mathrm{NMR}$ (126 MHz, $\mathrm{D_2O}$): δ 162.6, 156.7, 152.10, 140.1, 139.9 (d, J = 13.5 Hz), 138.7, 129.7, 129.6, 129.4, 128.1, 126.2, 125.3, 118.1, 112.9, 52.4 (d, J = 138.2 Hz), 38.1, 20.2. HRMS-ESI (m/z) [M — H^+] calcd for $\mathrm{C_{21}H_{19}N_3O_3PS}$: 424.0890, found 424.0878.

(*R*)- or (*S*)-(2-(3-Fluorophenyl)-1-((6-(p-tolyl)thieno[2,3-d]-pyrimidin-4-yl)amino)ethyl)phosphonic Acid [(*R*)- or (*S*)-**6e**]. Both compounds were isolated as off-white solids: (*R*)-**6e**, 6 mg, 40% yield; (*S*)-**6e**, 5 mg, 45% yield (yields indicated are for the last deprotection step). ¹H NMR (500 MHz, D₂O): δ 7.71 (s, 1H), 7.61 (s, 1H), 7.49 (d, *J* = 7.9 Hz, 2H), 7.14 (d, *J* = 7.7 Hz, 2H), 6.90 (dd, *J* = 16.5, 9.5 Hz, 3H), 6.60 (t, *J* = 8.4 Hz, 1H), 4.38 (ddd, *J* = 15.6, 12.1, 3.1 Hz, 1H), 3.27 (d, *J* = 13.6 Hz, 1H), 2.73 (td, *J* = 12.9, 6.5 Hz, 1H), 2.23 (s, 3H). ¹⁹F{¹H}NMR (471 MHz, D₂O): δ -115.07. ³¹P{¹H}NMR (203 MHz, D₂O): δ 15.62. ¹³C{¹H}NMR (126 MHz, D₂O): δ 163.3, 162.1 (d, *J* = 187.3 Hz), 156.8, 152.2, 142.6 (d, *J* = 21.2 Hz), 140.3, 139.0, 129.8, 129.6 (d, *J* = 8.4 Hz), 129.5, 125.6, 125.5, 118.2, 116.2 (d, *J* = 21.0 Hz), 113.1, 112.7 (d, *J* = 20.6 Hz), 52.3 (d, *J* = 136.6 Hz), 38.0, 20.3. HRMS-ESI (*m*/*z*) [M + H]⁺ calcd for C₂₁H₂₀FN₃O₃PS: 444.0942, found 444.0949.

(R)- or (S)-(1-((6-(3-Chloro-4-methylphenyl))thieno[2,3-d]-pyrimidin-4-yl)amino)-2-phenylethyl)phosphonic Acid [(R)- or (S)-**6f**]. Both compounds were isolated as off-white solids: (R)-**6f**, 18 mg, 90% yield; (S)-**6f**, 8 mg, 88% yield (yields indicated are for the last deprotection step). 1 H NMR (500 MHz, D_2O): δ 7.84 (s, 1H), 7.65 (s, 1H), 7.50 (s, 1H), 7.34 (d, J = 7.5 Hz, 2H), 7.25 (d, J = 7.9 Hz, 1H), 7.12 (t, J = 7.5 Hz, 2H), 7.03 (t, J = 7.3 Hz, 1H), 6.92 (d, J = 8.0 Hz, 1H), 4.58 (t, J = 13.7 Hz, 1H), 3.44 (d, J = 13.8 Hz, 1H), 2.90 (td, J = 12.7, 6.1 Hz, 1H), 2.18 (s, 3H). 31 P{ 1 H}NMR (203 MHz, D_2O): δ 15.79. 13 C{ 1 H}NMR (126 MHz, D_2O): δ 162.9, 156.7, 152.5, 139.8 (d, J = 7.1 Hz), 138.4, 135.9, 134.0, 131.6, 131.0, 129.4, 128.1, 126.1, 125.3, 123.5, 117.9, 113.8, 52.3 (d, J = 143.0 Hz), 38.0, 18.8. HRMS-ESI (m/z) [M - H $^{+}$] calcd for C_{21} H $_{18}$ ClN $_{3}$ O $_{3}$ PS: 458.0501, found 458.0489.

(R)- or (S)-(1-((6-(3-Chloro-4-methylphenyl)thieno[2,3-d]pyrimidin-4-yl)amino)-2-(3-fluorophenyl)ethyl)phosphonic Acid [(R)- or (S)-6g]. Both compounds were isolated as off-white solids: (R)-6g, 10 mg, 41% yield; (S)-6g, 5 mg, 50% yield (yields indicated are for the last deprotection step). ¹H NMR (400 MHz, D_2O): δ 7.88 (s, 1H), 7.79 (d, $\hat{J} = 1.5$ Hz, 2H), 7.58 (dd, $\hat{J} = 8.0$, 1.8 Hz, 1H), 7.37 (d, J = 8.0 Hz, 1H), 7.10-7.00 (m, 3H), 6.75 (t, J = 9.0 Hz, 1H), 4.53(ddd, J = 15.6, 12.3, 3.0 Hz, 1H), 3.42 (dt, J = 13.3, 3.0 Hz, 1H), 2.88(td, J = 13.3, 6.6 Hz, 1H), 2.41 (s, 3H). ${}^{31}P{}^{1}H{}NMR$ (162 MHz, D_2O): δ 15.31. ¹⁹F{¹H}NMR (377 MHz, D_2O) δ -115.57. ¹³C-{\text{1H}}NMR (126 MHz, D₂O): δ 163.0, 162.3 (d, J = 242.4 Hz), 156.9 (d, J = 6.6 Hz), 152.5, 142.6 (dd, J = 13.6, 7.2 Hz), 138.4, 136.3,134.2, 131.9, 131.2, 129.5 (d, J = 8.5 Hz), 125.6, 125.6 (d, J = 2.4Hz), 123.8, 117.9, 116.2 (d, J = 20.8 Hz), 114.1, 112.7 (d, J = 21.0Hz), 52.2 (d, J = 138.4 Hz), 38.0, 18.8. HRMS-ESI (m/z) $[M - H^{+}]^{-}$ calcd for C₂₁H₁₇ClFN₃O₃PS: 476.0406, found 476.0387.

(*R*)- or (*S*)-(1-((*6*-(3-Chloro-4-methylphenyl)thieno[2,3-d]-pyrimidin-4-yl)amino)-2-cyclohexylethyl)phosphonic Acid [(*R*)- or (*S*)-**6h**]. Both compounds were isolated as off-white solids: (*R*)-**6h**, 3 mg, 50% yield; (*S*)-**6h**, 5 mg, 35% yield (yields indicated are for the last deprotection step). ¹H NMR (500 MHz, D₂O): δ 8.21 (s, 1H), 7.59 (s, 1H), 7.47 (s, 1H), 7.34 (d, *J* = 7.9 Hz, 1H), 7.17 (d, *J* = 7.9 Hz, 1H), 4.43 (t, *J* = 13.7 Hz, 1H), 2.16 (s, 3H), 2.01 (d, *J* = 12.2 Hz, 1H), 1.81 (t, *J* = 12.4 Hz, 1H), 1.72–1.55 (m, 5H), 1.31 (d, *J* = 11.8 Hz, 1H), 1.22–1.01 (m, 4H), 0.92 (q, *J* = 11.8 Hz, 1H). ³¹P{¹H}-NMR (202 MHz, D₂O): δ 17.32. ¹³C{¹H}NMR (201 MHz, D₂O): δ 163.1, 153.2, 138.2, 136.3, 134.3, 132.0, 131.3, 125.7, 123.9, 114.2, 48.5, 47.8, 39.5, 34.2, 32.1, 26.2, 25.9, 18.9. HRMS-ESI (*m*/*z*) [M – H⁺]⁻ calcd for C₂₁H₂₅ClN₃O₃PS: 464.0970, found 464.0982.

((R)- or (S)-2-((6-(3-Chloro-4-methylphenyl)thieno[2,3-d]pyrimidin-4-yl)amino)-3-(3-fluorophenyl)propanoic Acid [(R)- or (S)-7b]. The S_NAr reaction between α -amino acid 17 and 14b was conducted based on a previously reported procedure with minor modifications. 8a,9 To a stirred solution of 14b (28 mg, 0.1 mmol, 1 equiv) in 1.6 mL of dioxane, HCl salt of 17 (33 mg, 0.15 mmol, 1.5 equiv) in dioxane: H_2O mixture (1:1, 1.6 mL, pH = \sim 8–9 adjusted with 2.5 equiv Na₂CO₃) was added. The mixture was stirred at 100 °C for 30 min and then acidified using 1 M HCl (10 mL). EtOAc (10 $mL \times 2$) was used to extract organic compounds from the aqueous phase. The crude was concentrated under reduced pressure. First purification was done by flash chromatography on silica gel using a solvent gradiant from 20 to 50% EtOAc in hexane followed by 0-10% MeOH in Et₂O. The concentrated polar fractions were repurified using semipreparative HPLC on a C18 reversed phase column (Atlantis T3 OBD Prep Column, 100 Å, 5 μ m, 19 mm × 50 mm) to give both enantiomers as white solids: (R)-7b (6 mg) in 20% yield, 80% ee; (S)-7b (15 mg) 32% yield, 83% ee. ¹H NMR (400 MHz, DMSO- d_6): δ 8.29 (s, 1H), 8.15 (s, 1H), 8.01 (d, J = 7.8 Hz, 1H), 7.74 (d, J = 1.9 Hz, 1H), 7.55 (dd, J = 7.9, 1.9 Hz, 1H), 7.47 (d, J =8.0 Hz, 1H), 7.26 (td, J = 8.0, 6.3 Hz, 1H), 7.16 - 7.09 (m, 2H), 7.00 -6.92 (m, 1H), 4.86 (q, J = 8.8, 7.5 Hz, 1H), 3.13 (dd, J = 13.9, 9.3 Hz,2H), 2.37 (s, 3H). 19 F{ 1 H}NMR (471 MHz, DMSO- d_6): δ –114.18. ¹³C{¹H}NMR (101 MHz, DMSO- d_6): δ 172.5, 164.9, 161.9 (d, J =242.3 Hz), 156.2, 154.0, 142.2 (d, J = 6.9 Hz), 136.1, 135.6, 134.1, 132.8, 132.0, 129.6 (d, J = 8.3 Hz), 125.4, 125.3 (d, J = 2.5 Hz), 124.3, 117.4, 116.0 (d, J = 10.8 Hz), 115.7, 112.6 (d, J = 20.8 Hz), 55.8, 36.9, 19.3. HRMS-ESI (m/z) [M + H]⁺ calcd for C₂₂H₁₇ClFN₃O₂S: 442.0787, found 442.0775. Chiral HPLC (UV abs 254 nm), Lux Cellulose-3 (250 mm × 4.6 mm), 60:40 MeCN:H₂O (0.1% formic acid), 1 mL/min: (R)-enantiomer t_R = 6.43 min, (S)-enantiomer $t_R = 6.81$ min.

Diethyl (1-Acetamidovinyl)phosphonate (8). The synthesis of compound 8 was achieved in two steps as previously reported. ^{18,25}

Step 1: Triethyl phosphite (9.2 mL, 54 mmol) was slowly added to acetyl chloride (3.8 mL, 60 mmol) at 0 °C under Ar. The mixture was stirred for 18 h at RT and concentrated under reduced pressure to remove excessive starting material and byproduct. Diethyl acetylphosphonate was isolated as a colorless oil (9.25 g, 95% yield). 1 H NMR (500 MHz, CDCl₃): δ 4.23 (p, J = 7.2 Hz, 4H), 2.48 (d, J = 5.1 Hz, 3H), 1.38 (t, J = 7.1 Hz, 6H). 31 P{ 1 H}NMR (203 MHz, CDCl₃): δ –2.89. NMR data consistent with those previously reported.

Step 2: In a 250 mL three-neck round-bottom flask connected to Dean–Stark apparatus with a condenser, cyclohexane (90 mL) was added to acetamide (4.35 g, 73.5 mmol, 1.5 equiv), pTsOH monohydrate (0.932 g, 4.9 mmol, 0.1 equiv), and p-methoxyphenol (6.1 mg, 0.049 mmol, 0.1 mol %) under Ar. The mixture was refluxed at 102 °C, and diethyl acetylphosphonate (9.29 g, 49 mmol) was added dropwise over 60 min with a syringe pump. After refluxing for another 2 h, the mixture was cooled to RT and concentrated. Water (100 mL) and EtOAc (50 mL) were added to the crude; the two phases were separated, and the aqueous phase was further extracted with EtOAc (50 mL × 2). The combined organic phase was dried over anhydrous MgSO₄ and concentrated. The crude pale-yellow oil was purified by flash chromatography using 20–85% EtOAc in hexane (desired product eluted at 60–70% EtOAc) to yield an off-white solid (1.6 g, 15% yield). ¹H NMR (500 MHz, CDCl₃): δ 7.18 (s, 1H), 6.66

(d, J = 41.6 Hz, 1H), 5.50 (d, J = 19.4 Hz, 1H), 4.18–4.07 (m, 4H), 2.10 (s, 3H), 1.35 (t, J = 7.1 Hz, 6H). 31 P{ 1 H}NMR (203 MHz, CDCl₃): δ 12.63. 13 C{ 1 H}NMR (126 MHz, CDCl₃): δ 169.5, 131.4 (d, J = 198.8 Hz), 113.3 (d, J = 9.2 Hz), 63.2 (d, J = 5.5 Hz), 24.8, 16.3 (d, J = 6.4 Hz). NMR data consistent with those previously reported. LRMS (ESI) m/z: 222.4 [M + H] $^{+}$.

Potassium 3-Fluorophenyl Trifluoroborate Salt (9d). The synthesis of trifluoroborate salt 9d was achieved using standard literature procedures.²⁶

Step 1: Anhydrous THF (15 mL) was added to an oven-dried 100 mL round-bottom flask under Ar, cooled to −78 °C, and n-BuLi (6 mL, 2.5 M in hexane, 20 mmol, 1.5 equiv) was added slowly. 3-Bromofluorobenzene (1.1 mL, 10 mmol, 1 equiv) was added dropwise, and the mixture was stirred for 30 min at -78 °C. Triisopropyl borate (4.6 mL, 20 mmol, 2 equiv) was added dropwise. Stirring was continued at -78 °C for an additional 20 min, and then the mixture was warmed up and stirred at RT for 30 min. HCl (1M, 15 mL) was subsequently added to hydrolyze the borate, and the mixture was stirred for 20 min. The aqueous phase was extracted with anhydrous Et₂O (30 mL \times 2). The combined organic phase was dried over anhydrous MgSO4 and concentrated. The crude solid was washed with hexane to remove any byproducts, and 3-fluorophenylboronic acid was isolated as a white solid (1 g, 65% yield), which was used as such in the following step. ¹H NMR (500 MHz, CDCl₃): δ 8.00 (d, J = 7.3 Hz, 1H), 7.88 (dt, J = 9.0, 4.6 Hz, 1H), 7.52 (m, 1H), 7.31 (m, 1H). 4.79 (s, boronic acid). ¹⁹F{¹H}NMR (471 MHz, CDCl₂): δ -113.53.

Step 2: 3-Fluorophenylboronic acid (0.62 g, 4.5 mmol, 1 equiv) was dissolved in MeOH (1.5 mL), and an excess of saturated KHF₂ aqueous solution (0.88 g in 2.5 mL of Milli-Q water, ~4.5 M, 11.3 mmol) was added slowly under vigorous stirring. After 30 min, the solvent was removed and the mixture was taken up in small quantity of MeCN and filtered to remove KHF₂. The filtrate was concentrated to obtain a white solid (0.89 g, quantitative yield), which was used directly in next step. ¹H NMR (400 MHz, DMSO- d_6): δ 7.11 (t, J = 5.0 Hz, 2H), 6.96 (dd, J = 10.2, 2.5 Hz, 1H), 6.83–6.74 (m, 1H). ¹⁹F{¹H}NMR (377 MHz, DMSO- d_6): δ -116.38. ¹³C{¹H}NMR (101 MHz, DMSO- d_6): δ 128.5 (d, J = 6.5 Hz), 127.5, 117.4 (d, J = 16.0 Hz), 111.8 (d, J = 20.8 Hz).

Diethyl (R)-(1-Acetamido-2-phenylethyl)phosphonate [(R)-10a]. The synthesis of (R)-10a was based on the procedure provided below for the preparation of (R)-10b with one modification; due to the poor solubility of potassium phenyl trifluoroborate in iPrOH, phenyl boronic acid was used instead. The desired product (R)-10a was isolated as a yellow oil (275 mg, 95% yield, 93% ee). ¹H NMR (400 MHz, CDCl₃): δ 7.34–7.25 (m, 4H), 7.24 (d, J = 6.8 Hz, 1H), 6.15 (d, J = 10.0 Hz, 1H), 4.79 (dtd, J = 16.3, 10.2, 4.9 Hz, 1H), 4.12 (m,4H), 3.24 (ddd, J = 14.0, 8.7, 4.9 Hz, 1H), 2.93 (dt, J = 14.4, 10.5 Hz, 1H), 1.90 (d, J = 1.1 Hz, 3H), 1.31 (t \times 2, J = 7.1 Hz, 6H). $^{31}P\{^{1}H\}NMR$ (162 MHz, CDCl₃): δ 24.21. $^{13}C\{^{1}H\}NMR$ (126 MHz, CDCl₃): δ 169.6 (d, J = 5.2 Hz), 136.7 (d, J = 12.8 Hz), 129.2, 128.5, 126.9, 63.0 (d, J = 6.9 Hz), 62.6 (d, J = 6.8 Hz), 46.8, 45.5, 35.8 (d, J = 3.3 Hz), 23.0, 16.5 (d × 2, J = 6.2 Hz). LRMS (ESI) m/z: 300.6 [M + H]+. Chiral HPLC (UV abs 220 nm) condition: Chiralcel OD (250 mm × 4.6 mm), 95:5 hexane:iPrOH, 0.8 mL/min; $t_R = 16.4$ min (major), 18.6 min (minor).

Diethyl (S)-(1-Acetamido-2-phenylethyl)phosphonate [(S)-10a]. Synthesis of (S)-10a was achieved using the procedure described below for the preparation of (S)-10b. The product was isolated as a yellow oil (115 mg) in 65% yield, 70% ee. $^1\mathrm{H}/^{31}\mathrm{P}/^{13}\mathrm{C}$ NMR and LC-MS data were identical to those of the (R)-isomer. Chiral HPLC (UV abs. 220 nm) condition: Chiralcel OD (250 mm × 4.6 mm), 95:5 hexane:iPrOH, 0.8 mL/min; $t_{\rm R}=16.7$ min (minor), 18.4 min (major).

Diethyl (R)-(1-Acetamido-2-(3-fluorophenyl)ethyl)phosphonate [(R)-10b]. Diethyl (1-acetamido-vinyl) phosphonate 8 (335 mg, 1.5 mmol, 1 equiv), potassium 3-fluorophenyl trifluoroborate 9d (576 mg, 2.85 mmol, 1.9 equiv), NaHCO₃ (252 mg, 3 mmol, 2 equiv), diμ-chloro-tetraethylene dirhodium(I) (8.8 mg, 0.023 mmol, 1.5 mol %), and (S)-difluorphos (33.8 mg, 0.05 mmol, 3.3 mol %) were

dissolved in anhydrous, degassed iPrOH (4 mL) under Ar in a microwave tube (Biotage), and the mixture was further degassed for 10 min with Ar. The resulting orange suspension was stirred at 90 °C for 20 h. After cooling to RT, saturated aqueous NH₄Cl solution (10 mL) was added into the mixture. The aqueous phase was extracted with DCM (10 mL \times 3); the combined organic phase was washed with brine and dried with anhydrous MgSO₄. The solvent was evaporated to yield crude product as brown viscous oil, which was purified by flash column chromatography on silica gel (from 1:1 EtOAc:hexane to 9:1 EtOAc:MeOH) to give the desired product as a yellow oil (330 mg, 70% yield, 90% ee). ¹H NMR (500 MHz, CDCl₃): δ 7.25 (m, 1H), 7.00 (d, J = 7.7 Hz, 1H), 6.92 (m, 2H), 5.65 (d, J = 10.1 Hz, NH), 4.75 (dd, J = 16.8, 4.9 Hz, 1H), 4.13 (m, 4H),3.20 (ddd, I = 14.4, 9.5, 4.9 Hz, 1H), 2.88 (dt, I = 14.6, 10.2 Hz, 1H), 1.91 (d, J = 0.8 Hz, 3H), 1.31 (t × 2, J = 7.1 Hz, 6H). $^{19}F\{^{1}H\}NMR$ (471 MHz, CDCl₃): δ –113.32. ³¹P{¹H}NMR (203 MHz, CDCl₃): δ 23.80. ¹³C{¹H}NMR (126 MHz, CDCl₃): δ 169.4 (d, I = 5.0 Hz), 139.2 (d, J = 5.4 Hz), 130.0 (d, J = 8.3 Hz), 124.9, 116.4 (d, J = 21.4Hz), 114.0 (d, J = 20.8 Hz), 63.0 (d, J = 7.1 Hz), 62.8 (d, J = 6.7 Hz), 46.6, 45.49, 35.7, 23.2, 16.5 (d \times 2, I = 5.5 Hz). LRMS (ESI) m/z: 318.3 [M + H]⁺. Chiral HPLC (UV abs 220 nm) condition: Chiralcel OD (250 mm × 4.6 mm), 95:5 hexane: iPrOH, 1 mL/min; $t_R = 12.3$ min (major), 15.1 min (minor)

Diethyl (S)-(1-Acetamido-2-(3-fluorophenyl)ethyl)phosphonate [(S)-10b]. Diethyl (1-acetamido-vinyl) phosphonate 8 (223 mg, 1 mmol, 1 equiv), 3-fluorophenyl boronic acid (280 mg, 2 mmol, 2 equiv), and Na₂CO₃ (106 mg, 1 mmol, 1 equiv) were mixed in dry and degassed dioxane (3 mL) under Ar in a microwave tube (Biotage). Bis(norbornadiene)rhodium(I) tetrafluoroborate (26 mg, 0.07 mmol, 7 mol %) and (S,S)-Chiraphos (32 mg, 0.075 mmol, 7.5 mol %) were premixed with degassed dioxane/water (0.9/0.45 mL) and injected into the microwave tube. The mixture was then further degassed for 10 min with Ar, and MeOH (0.32 mL, 8 equiv) was added dropwise. The orange suspension was heated to 70 °C for 20 h (monitored by TLC). After cooling to RT, solvent was removed under reduced pressure. The residue was redissolved in DCM, washed with water and brine, and dried over anhydrous MgSO4 to give the crude product as a brown viscous oil, which was purified by flash column chromatography on silica gel (using a solvent gradient from 1:1 EtOAc:hexane to 9:1 EtOAc:MeOH). Compound (S)-10b was isolated as a yellow oil (0.23 g) 70% yield in 89% ee. $^1H/^{19}F/^{31}P/^{13}C$ NMR and LC-MS data were identical to those of the (*R*)-enantiomer. Chiralcel OD (250 mm × 4.6 mm), 95:5 hexane:iPrOH, 1 mL/min; $t_{\rm R} = 12.7 \, \text{min (minor)}, \, 14.9 \, \text{min (major)}$

Diethyl (S)- or (R)-(1-Benzamido-2-cyclohexylethyl)phosphonate [(S)- or (R)-10c].²¹ Diethylzinc (0.15 mL, 1.3 M in toluene, 0.2 mmol) was added slowly to a stirred solution of (R,R) or (S,S)-ProPhenol (ligand L1; 64 mg, 0.1 mmol) in toluene (1.85 mL) under Ar. The mixture was stirred at RT for 0.5 h to generate zinc catalyst (0.05 M). The resulting catalyst solution (1 mL, 0.05 mmol) was added in one portion to freshly made 11 (120 mg, 0.5 mmol, ca. 80% purity) and diethyl phosphite (0.05 mL, 0.6 mmol, 1.2 equiv) in toluene (4 mL) at 0 °C under Ar. After stirring for 30 min, the reaction was quenched with saturated aqueous NH₄Cl solution. After extraction with anhydrous Et₂O (20 mL \times 2), the combined organic phase was washed with brine, dried over anhydrous MgSO₄, and concentrated under reduced pressure. The crude mixture was purified by flash column chromatography on silica gel using 20%-70% EtOAc in hexane to obtain (R)-10c or (S)-10c as a white solids (50 mg, 30%)yield for both enantiomers) with >95% ee (after recrystallization using DCM-pentane at -20 °C) and side product 12 (due to isomerization of starting material 11). ¹H NMR (400 MHz, CDCl₃): δ 7.81–7.74 (m, 2H), 7.57-7.49 (m, 1H), 7.49-7.41 (m, 2H), 6.10 (d, J = 10.1)Hz, 1H), 4.86-4.71 (m, 1H), 4.24-4.03 (m, 4H), 1.94 (d, J = 12.9Hz, 1H), 1.84–1.67 (m, 1H), 1.66 (m, 6H), 1.44–1.35 (m, 1H), 1.35 (s, 1H), 1.35-1.24 (m, 6H), 1.17 (m, 2H), 1.09-0.94 (m, 1H), 0.89 (t, J = 11.9 Hz, 1H). ³¹P {¹H} NMR (202 MHz, CDCl₃): δ 25.55. ¹³C { 1 H} NMR (126 MHz, CDCl₃): δ 167.0, 134.3, 131.9, 128.9, 127.1, 62.8 (dd, J = 19.2, 6.8 Hz), 42.9, 37.4, 34.1 (d, J = 12.7 Hz), 26.6, 26.1, 16.6 (d × 2, J = 5.8 Hz). LRMS (ESI) m/z: 368.3 [M + H]⁺.

HPLC (UV abs. 220 nm) condition: Chiralcel OD (250 mm \times 4.6 mm), 98:2 hexane:iPrOH, 0.8 mL/min; (R)-enantiomer t_R = 10.3 min (major), 12.9 min (minor); (S)-enantiomer t_R = 9.9 min (minor), 12.0 min (major).

(E)-N-(2-Cyclohexylethylidene)benzamide (11). The synthesis of 11 was achieved in three steps using the procedure recently reported by Lupton²⁷ with minor modifications.

Step 1: Pyridinium chlorochromate (3.23 g, 15 mmol, 1.5 equiv) was added in one portion to cyclohexylethanol (1.4 mL, 10 mmol) in DCM (50 mL), and the mixture was stirred at RT for 2 h. Silica gel (3.75 g) and anhydrous diethyl ether (50 mL) were subsequently added and stirring was continued for an additional 1 h. The mixture was concentrated, and the solid residue was loaded directly onto a silica gel column and eluted using 0%–25% EtOAc in hexane to yield the 2-cyclohexylacetaldehyde as a colorless oil (0.83 g, 63% yield). 1 H NMR (500 MHz, CDCl₃): δ 9.75 (t, J = 2.4 Hz, 1H), 2.28 (dd, J = 6.8, 2.4 Hz, 2H), 1.88 (m, 1H), 1.71 (m, 5H), 1.29 (m, 2H), 1.17 (m, 1H), 1.00 (m, 2H). 13 C{ 1 H}NMR (126 MHz, CDCl₃): δ 203.2, 51.5, 33.4, 32.8, 26.2.

Step 2: Benzenesulfinic acid sodium salt (2.73 g, 15 mmol, 1.5 equiv) and benzamide (1.82 g, 15 mmol, 1.5 equiv) were mixed with acetonitrile (100 mL) under Ar. After purging Ar for 15 min, 2cyclohexylacetaldehyde (1.41 g, 10 mmol) was added to the slurry in one portion. The suspension was cooled to 0 °C, and chlorotrimethylsilane (2.68 mL, 20 mmol, 2 equiv) was added slowly. The reaction was warmed up to RT and stirred for 16 h. Water (80 mL) was added to the suspension, and the mixture was stirred for 30 min. N-(2-Cyclohexyl-1-tosylethyl)benzamide precipitated as fine white solid and collected by filtration. The product was used in the next step without further purification (3.0 g, 80% yield). ¹H NMR (500 MHz, CDCl₃): δ 7.79–7.72 (m, 2H), 7.61–7.55 (m, 2H), 7.55-7.50 (m, 1H), 7.46-7.38 (m, 2H), 7.25-7.23 (m, 1H), 6.35 (d, I = 10.5 Hz, 1H), 5.52 (ddd, I = 11.7, 10.5, 3.1 Hz, 1H), 2.39 (s, 3H), $2.19 \text{ (ddd, } J = 14.2, 9.8, 3.1 \text{ Hz, } 1\text{H}), 1.89 - 1.78 \text{ (m, } 2\text{H}), 1.69 \text{ (d, } J = 1.89 - 1.89 \text{ (d, } J = 1.89 \text{ (d, } J = 1.89 - 1.89 \text{ (d, } J = 1.89 \text{ (d, } J = 1.89 - 1.89 \text{ (d, } J = 1.89 \text{$ 11.0 Hz, 3H), 1.62 (d, *J* = 6.9 Hz, 1H), 1.41 (dddt, *J* = 14.4, 10.8, 7.2, 3.7 Hz, 1H), 1.29-1.00 (m, 4H), 0.95 (tt, J = 12.0, 5.9 Hz, 1H). 13 C{ 1 H}NMR (101 MHz, CDCl₃): δ 166.4, 145.3, 133.8, 133.2, 132.4, 129.9, 129.2, 128.9, 127.1, 67.6, 34.2, 34.0, 33.9, 32.0, 26.4, 26.3, 26.0, 21.9. LRMS (ESI) m/z: 408.3 [M + Na]⁺.

Step 3: Cs₂CO₃ (2.45 g,7.5 mmol) and Na₂SO₄ (1.06 g, 7.5 mmol) were flame-dried under high vacuum, cooled under Ar, and mixed with anhydrous DCM (20 mL). N-(2-Cyclohexyl-1-tosylethyl)-benzamide (577 mg, 1.5 mmol) was added as DCM solution (5 mL). The reaction mixture was stirred vigorously (>1000 rpm) at RT for 4 h. Pentane (40 mL) was added to the mixture, and the solid was filtered. The solution was concentrated under reduced pressure at 20 °C to obtain 11 as colorless oil, which was used directly in the next step without purification. ¹H NMR (400 MHz, CDCl₃): δ 8.12 (t, J = 5.0 Hz, 1H), 8.06–7.98 (m, 2H), 7.61–7.54 (m, 1H), 7.46 (dd, J = 8.4, 7.0 Hz, 2H), 2.35 (dd, J = 6.5, 5.0 Hz, 2H), 1.86–1.59 (m, 7H), 1.36–1.13 (m, 3H), 1.11–0.98 (m, 2H). 13 C{ 1 H}NMR (101 MHz, CDCl₃): δ 180.9, 169.7, 133.5, 132.9, 130.0, 128.6, 77.5, 77.2, 76.8, 44.1, 35.3, 33.4, 26.3, 26.2. LRMS (ESI) m/z: 230.2 [M + H] $^{+}$.

(*E*)-*N*-(2-Cyclohexylvinyl)benzamide (12). Compound 12 was isolated as a white solid as major byproduct in the preparation of 10c. 1 H NMR (500 MHz, CDCl₃): δ 7.92–7.72 (m, 2H), 7.61 (d, J = 9.8 Hz, 1H), 7.58–7.47 (m, 1H), 7.44–7.38 (m, 2H), 6.94 (ddd, J = 14.4, 10.5, 1.3 Hz, 1H), 5.27 (dd, J = 14.4, 7.1 Hz, 1H), 2.04 (qdd, J = 8.1, 4.2, 1.2 Hz, 1H), 1.79–1.72 (m, 5H), 1.66 (dddt, J = 12.9, 5.1, 3.4, 1.6 Hz, 2H), 1.28 (tt, J = 12.7, 3.2 Hz, 2H), 1.23–1.16 (m, 1H), 1.16–1.08 (m, 2H).

General Procedure for the Synthesis of α-Aminophosphonate Diethyl Esters 13. A typical procedure for the N-deacetylation of intermediate 10 (regardless stereochemistry) at 1 mmol scale was achieved in three steps according to literature procedure.²³

Step 1: Intermediate 10 in anhydrous THF (4.5 mL) was transferred to a 10 mL microwave tube loaded with Boc₂O (437 mg, 2 mmol, 2 equiv) and DMAP (24 mg, 0.2 mmol, 0.2 equiv) under Ar. The tube was sealed, and the reaction mixture was stirred for 4 h at 80 °C. After cooling to RT, the solvent was removed under reduced

pressure, and the crude product was redissolved in DCM. The organic phase was washed with saturated aqueous NH₄Cl and NaHCO₃ solutions, dried over anhydrous Na₂SO₄, and concentrated to give crude as orange to brown oil.

Step 2: The crude from step 1 was diluted in THF—water mixture (2:1, in total 6 mL), and LiOH·H₂O (84 mg, 2 mmol, 2 equiv) was added. The suspension was stirred for 20–24 h at RT. The crude was diluted with anhydrous Et₂O (10 mL) and washed with 1 M HCl (4 mL) followed by brine. The organic phase was dried over anhydrous Na₂SO₄ and concentrated to give orange oil.

Step 3: The crude from step 2 was diluted in anhydrous DCM (8 mL) under Ar. HCl (4 M in dioxane, 5 mL, 20 equiv) was added dropwise to the solution. The mixture was stirred at RT for 2–4 h and monitored by TLC. After completion, the solvent was removed under reduced pressure and slowly taken up in 5% MeOH in DCM (10 mL). The solvent was removed again after stirring for 5 min, and the residue was redissolved in DCM. The organic phase was washed with 1 M NaOH (25 mL), followed by brine, and dried over anhydrous Na₂SO₄. The solution was concentrated to give light-orange oil. The crude product was purified by flash column chromatography on silica gel (from 1:1 EtOAc:hexane to 1.5:8.5 MeOH:EtOAc to yield light-yellow oil (50–80% isolated yield over three steps).

Diethyl (R)- or (S)-(1-Amino-2-phenylethyl)phosphonate [(R)- or (S)-13a]. Light-yellow oils (130–140 mg, ~50% yield). ¹H NMR (500 MHz, CDCl₃): δ 7.33–7.29 (m, 2H), 7.25–7.21 (m, 3H), 4.17 (dqd, J = 8.0, 7.0, 4.3 Hz, 4H), 3.31–3.18 (m, 2H), 2.66 (ddd, J = 13.9, 10.8, 9.1 Hz, 1H), 1.34 (t × 2, J = 7.1 Hz, 6H). ³¹P{¹H} NMR (203 MHz, CDCl₃): δ 28.01. ¹³C{¹H}NMR (126 MHz, CDCl₃): δ 138.1 (d, J = 16.0 Hz), 129.4, 128.7, 126.97, 62.4 (t, J = 7.5 Hz), 50.5 (d, J = 154.2 Hz), 38.0, 16.7 (d, J = 5.6 Hz). LRMS (ESI) m/z: 258.2 [M + H]⁺.

Diethyl (R)- or (S)-(1-Amino-2-(3-fluorophenyl)ethyl)-phosphonate [(R)- or (S)-13b]. Light-yellow oils (~130 mg, ~50% yield). ¹H NMR (500 MHz, CDCl₃): δ 7.29 (dd, J = 7.9, 6.1 Hz, 1H), 7.02 (d, J = 7.7 Hz, 1H), 6.95 (ddd, J = 10.7, 9.0, 2.3 Hz, 2H), 4.18 (qd, J = 7.0, 3.0 Hz, 4H), 3.26 (dd, J = 10.7, 3.3 Hz, 1H), 3.20 (dd, J = 13.9, 3.5 Hz, 1H), 2.68 (dd, J = 13.9, 10.9 Hz, 1H), 1.35 (t × 2, J = 7.1 Hz, 6H). ¹⁹F{¹H}NMR (471 MHz, CDCl₃): δ -113.21. ³¹P-{¹H}NMR (203 MHz, CDCl₃): δ 27.56. ¹³C{¹H}NMR (126 MHz, CDCl₃): δ 163.1 (d, J = 245.8 Hz), 140.7 (d, J = 7.3 Hz), 130.1 (d, J = 8.4 Hz), 125.1 (d, J = 2.8 Hz), 116.3 (d, J = 21.1 Hz), 113.8 (d, J = 21.1 Hz), 62.6 (d, J = 7.0 Hz), 62.5 (d, J = 7.0 Hz), 50.3 (d, J = 153.6 Hz), 37.8, 16.7 (d, J = 5.6 Hz). LRMS (ESI) m/z: 276.3 [M + H]⁺.

Diethyl (R)- or (S)-(1-Amino-2-cyclohexylethyl)phosphonate [(R)-or (S)-13c]. Light-yellow oils (~30 mg, ~80% yield). 1 H NMR (400 MHz, CDCl₃): δ 4.27–4.05 (m, 4H), 3.07 (td, J = 11.0, 3.2 Hz, 1H), 1.83–1.60 (m, 7H), 1.48–1.37 (m, 1H), 1.34 (t x 2, J = 7.1 Hz, 6H), 1.31–1.08 (m, 3H), 1.05–0.93 (m, 1H), 0.91–0.77 (m, 1H). 31 P{ 1 H}NMR (162 MHz, CDCl₃): δ 29.98. 13 C{ 1 H}NMR (126 MHz, CDCl₃): δ 62.2 (dd, J = 10.5, 7.3 Hz), 46.6, 45.5, 38.6, 34.4, 33.6 (d, J = 13.1 Hz), 32.0, 26.7, 26.5, 26.2, 16.7 (d, J = 5.5 Hz). LRMS (ESI) m/z: 264.3 [M + H] $^{+}$.

4-Fluoro-6-(p-tolyl)thieno[2,3-d]pyrimidine (14a) and 6-(3-Chloro-4-methylphenyl)-4-fluorothieno[2,3-d]pyrimidine (14b). The preparation and characterization of 14a and 14b were previously reported.⁹

General Procedure for the Synthesis of Aminophosphonate Esters 15d-h. The S_N Ar reaction between α -aminophosphonates 13 and scaffolds 14 was previously reported.

Diethyl (R)- or (S)-(2-Phenyl-1-((6-(p-tolyl)thieno[2,3-d]-pyrimidin-4-yl)amino)ethyl)phosphonate [(R)- or (S)- 15d]. Both enantiomers were isolated as off-white solids: (R)-15d in 47% yield (9 mg) and 90% ee and (S)-15d in 67% yield (21 mg) and 71% ee. 1 H NMR (400 MHz, CDCl₃): δ 8.37 (s, 1H), 7.53 (dd, J = 5.6, 2.7 Hz, 3H), 7.34–7.27 (m, 2H), 7.24–7.16 (m, 4H), 7.16–7.10 (m, 1H), 6.50 (s, 1H), 5.55–5.43 (m, 1H), 4.26–3.93 (m, 4H), 3.38 (ddd, J = 13.9, 8.6, 5.0 Hz, 1H), 3.29–3.14 (m, 1H), 2.38 (s, 3H), 1.31 (t, J = 7.0 Hz, 3H), 1.11 (t, J = 7.0 Hz, 3H). 31 P{ 1 H}NMR (162 MHz, CDCl₃): δ 24.18. 13 C{ 1 H}NMR (126 MHz, CDCl₃): δ 166.1, 156.2 (d, J = 5.0 Hz), 153.4, 141.2, 138.8, 136.9 (d, J = 12.7 Hz), 131.0,

129.8 (d, J = 2.2 Hz), 129.32 (d, J = 3.5 Hz), 128.5, 126.9, 126.4, 126.3, 118.2, 112.5, 63.5 (d, J = 6.9 Hz), 62.5 (d, J = 7.3 Hz), 47.3 (d, J = 156.2 Hz), 36.2 (d, J = 4.1 Hz), 21.4, 16.5 (d × 2, J = 5.8 Hz). LRMS (ESI) m/z: 482.4 [M + H]⁺. Chiral HPLC (UV abs 254 nm) condition: Chiralcel OD (250 mm × 4.6 mm), 90:10 hexane:iPrOH, 1 mL/min; (R)-enantiomer $t_R = 7.0$ min (minor), 15.0 min (major), (S)-enantiomer $t_R = 6.9$ min (major), 15.2 min (minor).

Diethyl (R)- or (S)-(2-(3-Fluorophenyl)-1-((6-(p-tolyl)thieno[2, 3d]pyrimidin-4-yl)amino)ethyl)phosphonate [(R)- or (S)-15e]. Both enantiomers were isolated as off-white solids: (R)-15e in 72% yield (21 mg) and 80% ee; (S)-15e in 50% yield (15 mg) and 86% ee. ¹H NMR (400 MHz, CDCl₃): δ 8.41 (s, 1H), 7.55 (d, J = 8.2 Hz, 2H), 7.31 (s, 1H), 7.24 (d, J = 8.0 Hz, 2H), 7.16 (td, J = 8.1, 6.1 Hz, 1H), 7.08-7.01 (m, 2H), 6.85 (ddd, I = 10.6, 8.1, 2.6 Hz, 1H), 5.58 (d, I = 10.6, 8.1, 2.69.9 Hz, 1H), 5.44 (dtd, J = 16.4, 9.7, 5.0 Hz, 1H), 4.23–3.95 (m, 4H), 3.37 (ddd, J = 14.7, 9.9, 5.0 Hz, 1H), 3.13 (dt, J = 14.6, 10.3 Hz, 1H),2.40 (s, 3H), 1.30 (t, J = 7.1 Hz, 3H), 1.17 (t, J = 7.1 Hz, 3H). ¹⁹F{¹H}NMR (377 MHz, CDCl₃): δ -113.33. ³¹P{¹H}NMR (162 MHz, CDCl₃): δ 23.87. ¹³C{¹H}NMR (126 MHz, CDCl₃): δ 166.1, 162.7 (d, J = 245.7 Hz), 156.1 (d, J = 5.0 Hz), 153.2, 141.1, 139.5(dd, J = 13.5, 7.4 Hz), 138.7, 130.9, 129.8 (d, J = 8.5 Hz), 129.7,126.2, 124.8 (d, *J* = 2.8 Hz), 118.1, 116.3 (d, *J* = 21.5 Hz), 113.7 (d, *J* = 21.0 Hz), 112.6, 63.0 (dd, J = 143.4, 7.1 Hz), 47.0 (d, J = 156.6Hz), 35.7 (d, J = 4.4 Hz), 21.3, 16.3 (d × 2, J = 5.9 Hz). LRMS (ESI) m/z: 500.4 [M + H]⁺. Chiral HPLC (UV abs. 254 nm) condition: Chiralcel OD (250 mm × 4.6 mm), 90:10 hexane:iPrOH, 1 mL/min: (R)-enantiomer $t_R = 5.8 \text{ min (minor)}$, 21.4 min (major), (S)enantiomer $t_R = 7.0 \text{ min (major)}$, 24.3 min (minor).

Diethyl (R)- or (S)-(1-((6-(3-Chloro-4-methylphenyl)thieno[2,3d]pyrimidin-4-yl)amino)-2-phenylethyl) phosphonate [(R)- or (S)-15f]. Both enantiomers were isolated as off-white solids: (R)-15f in 76% yield (26 mg) and 92% ee; (S)-15f in 44% yield (11 mg) and 71% ee. ¹H NMR (500 MHz, CDCl₃): δ 8.37 (s, 1H), 7.63 (d, J = 2.0Hz, 1H), 7.61 (s, 1H), 7.41 (dd, J = 7.9, 2.0 Hz, 1H), 7.31 (d, J = 7.0Hz, 2H), 7.24 (d, J = 7.8 Hz, 1H), 7.19 (t, J = 7.5 Hz, 2H), 7.13 (m, 1H), 5.50 (dtd, J = 14.9, 9.9, 4.8 Hz, 1H), 4.27–3.91 (m, 2H), 3.39 (ddd, J = 13.5, 8.3, 4.8 Hz, 1H), 3.25 (dt, J = 14.4, 10.6 Hz, 1H), 2.40(s, 3H), 1.33 (t, J = 7.1 Hz, 3H), 1.10 (t, J = 7.0 Hz, 3H). $^{31}P\{^{1}H\}NMR$ (203 MHz, CDCl₃): δ 24.16. $^{13}C\{^{1}H\}NMR$ (126 MHz, CDCl₃): δ 166.1, 156.2 (d, J = 4.9 Hz), 153.4, 141.2, 138.8, 136.9 (d, J = 12.7 Hz), 131.0, 129.8 (d, J = 2.2 Hz), 129.3 (d, J = 3.5Hz), 128.5, 126.9, 126.4, 126.3, 118.2, 112.5, 63.5 (d, J = 6.9 Hz), 62.5 (d, J = 7.3 Hz), 47.3 (d, J = 156.2 Hz), 36.2 (d, J = 4.1 Hz), 21.4, 16.5 (d × 2, J = 5.8 Hz). LRMS (ESI) m/z: 517.3 [M + H]⁺. Chiral HPLC (UV abs 254 nm), Chiralcel OD (250 mm × 4.6 mm), 90:10 hexane: iPrOH, 1 mL/min: (R)-enantiomer $t_R = 5.5$ min (minor), 12.3 min (major); (S)-enantiomer $t_R = 5.5$ min (major), 12.2 min (minor).

Diethyl(R)- or (S)-(1-((6-(3-Chloro-4-methylphenyl)thieno[2,3-d]pyrimidin-4-yl)amino)-2-(3-fluorophenyl)ethyl)phosphonate [(R)or (S)-15g]. Both enantiomers were isolated as off-white solids: (R)-15g in 44% yield (25 mg) and 78% ee; (S)-15g in 26% yield (14 mg) and 87% ee. 1 H NMR (400 MHz, CDCl₃): δ 8.41 (s, 1H), 7.65 (d, J = 1.8 Hz, 1H), 7.43 (dd, J = 7.9, 1.8 Hz, 1H), 7.35 (s, 1H), 7.28(d, J = 8.3 Hz, 1H), 7.21–7.13 (m, 1H), 7.04 (t, J = 9.3 Hz, 2H), 6.85 (td, J = 8.6, 1.9 Hz, 1H), 5.64 (d, 1H), 5.44 (dtd, J = 19.6, 9.7, 4.9 Hz,1H), 4.28–3.98 (m, 4H), 3.38 (ddd, *J* = 14.3, 9.6, 4.6 Hz, 1H), 3.13 (dt, J = 14.3, 10.3 Hz, 1H), 2.41 (s, 3H), 1.31 (t, J = 7.1 Hz, 3H), 1.17(t, J = 7.0 Hz, 3H). $^{19}F\{^{1}H\}NMR$ (471 MHz, CDCl₃): $\delta - 113.29$. $^{31}P\{^{1}H\}NMR$ (162 MHz, CDCl₃): δ 23.79. $^{13}C\{^{1}H\}NMR$ (126 MHz, CDCl₃): δ 166.4, 162.8 (d, J = 245.8 Hz), 156.4 (d, J = 4.7 Hz), 153.7, 139.6 (dd, *J* = 13.7, 7.4 Hz), 139.3, 136.5, 135.1, 133.2, 131.6, 129.9 (d, J = 8.2 Hz), 126.6, 124.9 (d, J = 2.8 Hz), 124.8, 118.1, 116.4 (d, J = 21.4 Hz), 113.8, 113.8 (d, J = 21.0 Hz), 63.8 (d, J = 6.9 Hz),62.6 (d, J = 7.3 Hz), 47.1 (d, J = 156.6 Hz), 35.8, 20.0, 16.6 (d, J = 6.0Hz), 16.3 (d, I = 6.0 Hz). LRMS (ESI) m/z: 534.4 [M + H]⁺. Chiral HPLC (UV abs. 254 nm): Chiralcel OD (250 mm × 4.6 mm), 90:10 hexane: iPrOH, 1 mL/min: (R)-enantiomer $t_R = 5.4 \text{ min (minor)}$, 20.8 min (major); (S)-enantiomer $t_R = 5.4$ min (major), 21.5 min (minor).

Diethyl(R)- or (S)-(1-((6-(3-Chloro-4-methylphenyl)thieno [2,3-d]pyrimidin-4-yl)amino)-2-cyclohexylethyl)phosphonate [(R)- or

(S)-15h]. Both enantiomers were isolated as off-white solids: (R)-15h in 60% yield (15 mg) and 99% ee; (S)-15h in 52% yield (13 mg) and 91% ee. ¹H NMR (500 MHz, CDCl₃): δ 8.45 (s, 1H), 7.69 (d, I = 4.3 Hz, 1H), 7.64 (d, I = 1.9 Hz, 1H), 7.42 (dd, I = 7.8, 1.9 Hz, 1.91H), 7.24 (d, I = 7.9 Hz, 1H), 6.58 (s, 1H), 5.34–5.22 (m, 1H), 4.28-4.07 (m, 3H), 2.39 (s, 4H), 1.91 (tt, J = 16.4, 7.6 Hz, 4H), 1.82-1.71 (m, 1H), 1.63-1.57 (m, 1H), 1.41 (s, 1H), 1.37-1.22 (m, 4H), 1.16-0.95 (m, 7H), 0.95-0.83 (m, 1H). ³¹P{¹H}NMR (203 MHz, CDCl₃): δ 25.55. ¹³C{¹H}NMR (126 MHz, CDCl₃): δ 166.4, 156.6 (d, *J* = 3.8 Hz), 154.0, 139.2, 136.5, 135.2, 133.1, 131.6, 126.6, 124.7, 118.0, 113.9, 63.3 (d, I = 7.0 Hz), 62.5 (d, I = 7.2 Hz), 43.8 (d, J = 155.7 Hz), 37.5, 34.2, 33.9 (d, J = 13.1 Hz), 32.2, 26.6, 26.3, 26.0, 20.0, 16.5 (d \times 2, J = 5.9 Hz). Chiral HPLC (UV abs 254 nm), Chiralcel OD (250 mm × 4.6 mm), 90:10 hexane:iPrOH, 1 mL/min: (R)-enantiomer $t_R = 5.3 \text{ min (minor)}$, 7.2 min (major); (S)enantiomer $t_R = 4.9 \text{ min (major)}$, 6.5 min (minor).

Methyl (*R*)-2-Acetamido-3-(3-fluorophenyl)propanoate [(*R*)-16]. ²⁴ Methyl-2-acetamidoacrylate (1 mmol, 146 mg), potassium 3-fluorophenyl trifluoroborate 9d (364 mg, 1.8 mmol, 1.8 equiv), bis(1,5-cyclooctadiene)rhodium(I) tetrafluoroborate (12.2 mg, 3 mol %), and (*S*)-BINAP (37 mg, 6 mol %) were mixed in degassed, anhydrous toluene (3 mL) under Ar. Freshly distilled guaiacol (74 μ L, 0.66 mmol, 1.2 equiv) was added, and the mixture was stirred at 110 °C for 16 h (monitored by TLC). After cooling to RT, the mixture was diluted with anhydrous Et₂O (10 mL) and directly dry-loaded into a silica gel column. The crude was purified using 10%–75% EtOAc in hexane to obtain white solid (118 mg, 50% yield, 85% ee). 1 H/ 19 F/ 13 C NMR and LC-MS data were identical to those of the (*S*)-isomer. Chiral HPLC (UV abs 220 nm), Chiralcel OD (250 mm × 4.6 mm), 90:10 hexane:*i*PrOH, 1 mL/min: (*S*)-enantiomer t_R = 10.3 min (minor), (*R*)-enantiomer t_R = 13.4 min (major).

Methyl (S)-2-Acetamido-3-(3-fluorophenyl)propanoate [(S)-**16].** Synthesis of (S)-16 was achieved using the procedure described for preparing (R)-10b. The crude product was purified by flash column chromatography on silica gel using a solvent gradient from 10 to 70% EtOAc in hexane to obtain the desired product as an off-white solid (125 mg, 67% yield, 81% ee). 1 H NMR (400 MHz, CDCl₃): δ 7.29-7.21 (m, 1H), 6.94 (tdd, I = 8.5, 2.7, 1.0 Hz, 1H), 6.87 (dt, I =7.6, 1.3 Hz, 1H), 6.80 (ddd, J = 9.7, 2.5, 1.6 Hz, 1H), 5.96 (d, J = 7.7Hz, 1H), 4.88 (dt, J = 7.7, 5.7 Hz, 1H), 3.74 (s, 3H), 3.12 (qd, J =13.9, 5.7 Hz, 2H), 2.00 (s, 3H). 19 F $\{^{1}$ H $\}$ NMR (377 MHz, CDCl₃): δ -112.99. 13 C 1 H 1 NMR (126 MHz, CDCl 3): δ 172.0, 169.7, 162.9 (d, J = 246.3 Hz), 138.5 (d, J = 7.3 Hz), 130.2 (d, J = 8.4 Hz), 125.1 (d, J = 8.4 Hz) = 2.9 Hz), 116.3 (d, J = 21.1 Hz), 114.2 (d, J = 20.9 Hz), 53.1, 52.6, 37.7 (d, J = 1.8 Hz), 23.29. LRMS (ESI) m/z: 240.2 [M + H]⁺. Chiral HPLC (UV abs 220 nm): (R)-enantiomer $t_R = 11.4 \text{ min (major)}$, (S)enantiomer $t_R = 14.8 \text{ min (minor)}$.

(R)- or (S)-2-Amino-3-(3-fluorophenyl)propanoic Acid [(R)or (S)-17]. The synthesis of 17 was achieved using the same procedure as for 13, however, in step 2, during LiOH hydrolysis, both the N-deacetylation and the ester hydrolysis take place to give the desired amino acid HCl salts as white solids; (R)-17 in 70% yield (41 mg) and (S)-17 in 74% yield (86 mg). The enantiomeric purity of amino acids 17 was not determined at this stage but assumed to be very similar to the final inhibitors (R)- and (S)-7b, which were analyzed by chiral HPLC and found to have 80% ee and 83% ee for (R) and (S), respectively. ¹H NMR (400 MHz, D₂O): δ 7.43 (td, J =7.9, 6.1 Hz, 1H), 7.22-7.06 (m, 3H), 4.30 (dd, J = 7.5, 5.8 Hz, 1H), 3.37 (dd, J = 14.7, 5.6 Hz, 1H), 3.23 (dd, J = 14.6, 7.7 Hz, 1H). 19 F{ 1 H}NMR (377 MHz, D₂O): δ -113.13. 13 C{ 1 H}NMR (126 MHz, D₂O): δ 171.7, 162.8 (d, J = 244.1 Hz), 136.7 (d, J = 7.5 Hz), 130.9 (d, J = 8.5 Hz), 125.2 (d, J = 2.8 Hz), 116.1 (d, J = 21.9 Hz), 114.7 (d, J = 21.1 Hz), 54.3, 35.4 (d, J = 1.8 Hz). LRMS (ESI) m/z: $184.2 [M + H]^{+}$

Expression and Purification of hFPPS. A plasmid (vector p11, SGC Oxford) encoding hFPPS with an N-terminal His-tag was transformed into *Escherichia coli* BL21 (DE3) cells. The cells were grown in LB at 37 °C until the OD₆₀₀ of 0.6 was reached. Expression of the recombinant protein was induced overnight at 18 °C in the presence of 1 mM IPTG. The cells were lysed in a buffer solution

composed of 50 mM HEPES, 500 mM NaCl, 5 mM β -mercaptoethanol, 5 mM imidazole, and 5% (v/v) glycerol (pH 7.5). The lysate was cleared of cell debris by centrifugation and applied to a metal ion affinity column (Ni-NTA Superflow Cartridge, Qiagen). Bound proteins were eluted with an increasing imidazole gradient, and the fractions containing hFPPS were pooled and applied to a size-exclusion column (HiLoad 26/60 Superdex 200, GE Healthcare). Imidazole was removed from the sample during the size-exclusion step, in which the running buffer consisted of 20 mM HEPES, 500 mM NaCl, 5 mM β -mercaptoethanol, and 5% (v/v) glycerol (pH 7.5). The purified sample was concentrated in a centrifugal concentrator (MWCO of 50000 Da) to the final concentration of 20 mg/mL and stored at 4 °C for later use.

In Vitro Inhibition Assay. Reactions were carried out with 2 μM GPP, 1.8 μ M IPP (containing ¹⁴C-IPP, 55 μ Ci/ μ mol), and 40 ng/mL of the purified enzyme in the final volume of 200 µL. The reaction mixture also contained 50 mM Tris (pH 7.7), 1 mM MgCl₂, 0.5 mM TCEP, 20 μ g/mL BSA, and 0.01% Triton X-100. Catalysis proceeded for 5 min at 37 °C after a preincubation period; the enzyme and inhibitor (if added) were incubated in the reaction mixture for 10 min before the substrates were added to initiate the reaction. The reactions were terminated by adding 400 µL of HCl/methanol (1:4) quenching solution, followed by an additional incubation of 10 min at 37 °C. The reaction product was extracted with 700 μ L of ligroin, and 350 μL of the ligroin phase were added to 8 mL of scintillation cocktail (EcoLite, MP Biomedicals). Radioactivity was measured with a Beckman Coulter LS6500 liquid scintillation counter. All reactions were carried out in triplicate, and the IC50 values were determined with the program GraFit (Erithacus Software).

Crystallization of Inhibitors Bound to hFPPS. Each compound was added to the purified protein sample to give final concentrations of 1.0 and 0.25 mM, respectively. Crystals were produced at 22 °C by vapor diffusion in hanging drops composed of 1 μ L of inhibitor/protein mixture and 1 μ L of crystallization solution. The composition of the crystallization solutions was as follows: 1.6 M (NH₄)₂HPO₄, 20% glycerol, and 0.08 M Tris (pH 8.5) for the crystals containing (R)- and (S)-6d and (R)-6g: 0.6 M KH₂PO₄, 0.6 M NaH₂PO₄, 25% glycerol, and 0.075 M HEPES (pH 7.5) for (R)- and (S)-6f, and 0.04 M KH₂PO₄, 16% PEG 8K, and 20% glycerol for (S)-6g.

X-ray Diffraction and Structure Refinement. Diffraction data were collected from single crystals under cryogenic conditions with either synchrotron radiation (Canadian Light Source, Saskatoon, SK) or a home source generator (MetalJet D2, Bruker). The synchrotron data sets were indexed and scaled with the xia2 program package, ²⁸ and the home source set with the Proteum3 software suite (Bruker). The initial structure models were built by difference Fourier methods with the PDB entry 4XQR or 4H5C as the starting template. The models were improved through iterative rounds of manual and automated refinement with COOT²⁹ and REFMAC5.³⁰ The final models were deposited to the PDB. The discovery maps for the bound inhibitors are presented in Supporting Information, Figure S1. Data collection and structure refinement statistics and the PDB IDs for the final structure models are summarized in Supporting Information, Table S1.

ASSOCIATED CONTENT

S Supporting Information

The Supporting Information is available free of charge on the ACS Publications website at DOI: 10.1021/acs.jmed-chem.9b01104.

¹H, ¹³C, ³¹P NMR spectra, and chiral HPLC chromatograms. X-ray data collection and structure refinement for cocrystal structures of both (*R*)- and (*S*)-enantiomers of inhibitors **6d**, **6f**, and **6g** (PDF)

Molecular formula strings and biological data (CSV)

Accession Codes

The PDB accession code for the X-ray cocrystal structures of hFPPS with inhibitors bound (*S*)-6d (PDB 6N7Z), (*R*)-6d (PDB 6N7Y), (*S*)-6f (PDB 6OAG), (*R*)-6f (PDB 6OAH), (*S*)-6g (PDB 6N82), (*R*)-6g (PDB 6N83). Authors will release the atomic coordinates and experimental data upon article publication.

AUTHOR INFORMATION

Corresponding Authors

*For Y.S.T.: phone, 514-398-3638; E-mail, Youla.tsantrizos@mcgill.ca.

*For A.M.B.: E-mail, Albert.berghuis@mcgill.ca.

ORCID ®

Jaeok Park: 0000-0002-8180-3950

Youla S. Tsantrizos: 0000-0002-6231-7498

Author Contributions

Y. F. and J. P. contributed equally; P.V. was an undergraduate research participant; conceptualization of project (Y.S.T.); synthesis of inhibitors (Y.F., S.-G. L., and P.V.); in vitro evaluation of inhibitors (J.P. and R.B.); X-ray crystallography (J.P and A.M.B.); Y.S.T. wrote the manuscript with contributions from all group members.

Notes

The authors declare no competing financial interest.

ACKNOWLEDGMENTS

We are very grateful for financial support from the Natural Sciences and Engineering Research Council of Canada (NSERC, grant no. RGPIN-2015-05529 to Y.S.T. and RGPIN-2019-05067 to A.M.B.).

■ ABBREVIATIONS USED

hFPPS, human farnesyl pyrophosphate synthase; FPP, farnesyl pyrophosphate; IPP, isopentenyl pyrophosphate; DMAPP, dimethyl allyl pyrophosphate; GGPP, geranylgeranyl pyrophosphate; N-BPs, nitrogen-containing bisphosphonates; C^6 -ThP-MP, C6-substituted thienopyrimidine-based monophosphonate

■ REFERENCES

- (1) (a) Dunford, J. E.; Thompson, K.; Coxon, F. P.; Luckman, S. P.; Hahn, F. M.; Poulter, C. D.; Ebetino, F. H.; Rogers, M. J. Structure-activity relationship for inhibition of farnesyl diphosphate synthase in vitro and inhibition of bone resorption in vivo by nitrogen-containing bisphosphonates. *J. Pharmacol. Exp. Ther.* **2001**, 296, 235–242. (b) Coxon, F. P.; Thompson, K.; Rogers, M. J. Recent advances in understanding the mechanism of action of bisphosphonates. *Curr. Opin. Pharmacol.* **2006**, 6, 307–312. (c) Eastell, R.; Walsh, J. S.; Watts, N. B.; Siris, E. Bisphosphonates for postmenopausal osteoporosis. *Bone* **2011**, 49, 82–88. (d) Ebetino, F. H.; Hogan, A.-M.; Sun, S.; Tsoumpra, M. K.; Duan, X.; Triffitt, J. T.; Kwaasi, A. A.; Dunford, J. E.; Barnett, B. L.; Oppermann, U.; Lundy, M. W.; Boyde, A.; Kashemirov, B. A.; McKenna, C. E.; Russell, R. G. The relationship between the chemistry and biological activity of the bisphosphonates. *Bone* **2011**, 49, 20–33.
- (2) (a) Berndt, N.; Hamilton, A. D.; Sebti, S. M. Targeting protein prenylation for cancer therapy. *Nat. Rev. Cancer* **2011**, *11*, 775–791. (b) Mullen, P. J.; Yu, R.; Longo, J.; Archer, M. C.; Penn, L. Z. The interplay between cell signalling and the mevalonate pathway in cancer. *Nat. Rev. Cancer* **2016**, *16*, 718–731.
- (3) Kavanagh, K. L.; Guo, K.; Dunford, J. E.; Wu, X.; Knapp, S.; Ebetino, F. H.; Rogers, M. J.; Russell, R. G.; Oppermann, U. The molecular mechanism of nitrogen-containing bisphosphonates as

antiosteoporosis drugs. *Proc. Natl. Acad. Sci. U. S. A.* **2006**, 103, 7829–7834.

- (4) (a) Morgan, G. J.; Davies, F. E.; Gregory, W. M.; Cocks, K.; Bell, S. E.; Szubert, A. J.; Navarro-Coy, N.; Drayson, M. T.; Owen, R. G.; Feyler, S.; Ashcroft, A. J.; Ross, F.; Byrne, J.; Roddie, H.; Rudin, C.; Cook, G.; Jackson, G. H.; Child, J. A. First-line treatment with zoledronic acid as compared with clodronic acid in multiple myeloma (MRC Myeloma IX): a randomized controlled trial. *Lancet* 2010, 376, 1989–1999. (b) Morgan, G. J.; Davies, F. E.; Gregory, W. M.; Szubert, A. J.; Bell, S. E.; Drayson, M. T.; Owen, R. G.; Ashcroft, A. J.; Jackson, G. H.; Child, J. A. Effects of induction and maintenance plus long-term bisphosphonates on bone disease in patients with multiple myeloma: the Medical Research Council Myeloma IX Trial. *Blood* 2012, 119, 5374–5383.
- (5) (a) Coleman, R. E.; Marshall, H.; Cameron, D.; Dodwell, D.; Burkinshaw, R.; Keane, M.; Gil, M.; Houston, S. J.; Grieve, R. J.; Barrett-Lee, P. J.; Ritchie, D.; Pugh, J.; Gaunt, C.; Rea, U.; Peterson, J.; Davies, C.; Hiley, V.; Gregory, W.; Bell, R. Breast-cancer adjuvant therapy with zoledronic acid. N. Engl. J. Med. 2011, 365, 1396-1405. (b) Gnant, M.; Mlineritsch, B.; Stoeger, H.; Luschin-Ebengreuth, G.; Heck, D.; Menzel, C.; Jakesz, R.; Seifert, M.; Hubalek, M.; Pristauz, G.; Bauernhofer, T.; Eidtmann, H.; Eiermann, W.; Steger, G.; Kwasny, W.; Dubsky, P.; Hochreiner, G.; Forsthuber, E. P.; Fesl, C.; Greil, R. Adjuvant endocrine therapy plus zoledronic acid in premenopausal women with early-stage breast cancer: 62-month follow-up from the ABCSG-12 randomised trial. Lancet Oncol. 2011, 12, 631-641. (c) Gnant, M.; Mlineritsch, B.; Schippinger, W.; Luschin-Ebengreuth, G.; Pöstlberger, S.; Menzel, C.; Jakesz, R.; Seifert, M.; Hubalek, M.; Bjelic-Radisic, V.; Samonigg, H.; Tausch, C.; Eidtmann, H.; Steger, G.; Kwasny, W.; Dubsky, P.; Fridrik, M.; Fitzal, F.; Stierer, M.; Rücklinger, E.; Greil, R. Endocrine therapy plus zoledronic acid in premenopaisal breast cancer. N. Engl. J. Med. 2009, 360, 679-691. (d) Coleman, R.; de Boer, R.; Eidtmann, H.; Llombart, A.; Davidson, N.; Neven, P.; von Minckwitz, G.; Sleeboom, H. P.; Forbes, J.; Barrios, C.; Frassoldati, A.; Campbell, I.; Paija, O.; Martin, N.; Modi, A.; Bundred, N. Zoledronic acid (zoledronate) for postmenopausal women with early breast cancer receiving adjuvant letrozole (ZO-FAST study): 60-months results. Ann. Oncol. 2013, 24, 398-405.
- (6) Jahnke, W.; Rondeau, J.-M.; Cotesta, S.; Marzinzik, A.; Pellé, X.; Geiser, M.; Strauss, A.; Götte, M.; Bitsch, F.; Hemmig, R.; Henry, C.; Lehmann, S.; Glickman, J. F.; Roddy, T. P.; Stout, S. J.; Green, J. R. Allosteric non-bisphosphonate FPPS inhibitors identified by fragment-based discovery. *Nat. Chem. Biol.* **2010**, *6*, 660–666.
- (7) Park, J.; Zielinski, M.; Magder, A.; Tsantrizos, Y. S.; Berghuis, A. M. Human farnesyl pyrophosphate synthase is allosterically inhibited by its own preoducts. *Nat. Commun.* **2017**, *8*, 14132.
- (8) (a) De Schutter, J. W.; Park, J.; Leung, C. Y.; Gormley, P.; Lin, Y.-S.; Hu, Z.; Berghuis, A. M.; Poirier, J.; Tsantrizos, Y. S. Multistage screening reveals chameleon ligands of the human farnesyl pyrophosphate synthase: implications to drug discovery for neurodegenerative diseases. J. Med. Chem. 2014, 57, 5764-5776. (b) Gritzalis, D.; Park, J.; Chiu, W.; Cho, H.; Lin, Y.-S.; De Schutter, J. W.; Lacbay, C. M.; Zielinski, M.; Berghuis, A. M.; Tsantrizos, Y. S. Probing the molecular and structural elements of ligands binding to the active site versus an allosteric pocket of the human farnesyl pyrophosphate synthase. Bioorg. Med. Chem. Lett. 2015, 25, 1117-1123. (c) Marzinzik, A. L.; Amstutz, R.; Bold, G.; Bourgier, E.; Cotesta, S.; Glickman, J. F.; Götte, M.; Henry, C.; Lehmann, S.; Hartwieg, J. C. D.; Ofner, S.; Pellé, X.; Roddy, T. P.; Rondeau, J.-M.; Stauffer, F.; Stout, S. J.; Widmer, A.; Zimmermann, J.; Zoller, T.; Jahnke, W. Discovery of novel allosteric nonbisphosphonate inhibitors of farnesyl pyrophosphate synthase by integrated lead finding. ChemMedChem 2015, 10, 1884-1891. (d) Liu, Y.-L.; Cao, R.; Wang, Y.; Oldfield, E. Farnesyl diphosphate synthase inhibitors with unique ligand-binding geometries. ACS Med. Chem. Lett. 2015, 6, 349-354.
- (9) Park, J.; Leung, C. Y.; Matralis, A. N.; Lacbay, C. M.; Tsakos, M.; Fernández De Troconiz, G.; Berghuis, A. M.; Tsantrizos, Y. S. Pharmacophore mapping of thienopyrimidine-based monophospho-

- nate (ThP-MP) inhibitors of the human farnesyl pyrophosphate synthase. J. Med. Chem. 2017, 60, 2119–2134.
- (10) For a recent review see: Mucha, A.; Kafarski, P.; Berlicki, Ł. Remarkable potential of the α -aminophosphonate/phosphinate structural motif in medicinal chemistry. *J. Med. Chem.* **2011**, *54*, 5955–5980.
- (11) (a) Pompei, M.; Di Francesco, M. E.; Koch, U.; Liverton, N. J.; Summa, V. Phosphorous acid analogs of novel P2-P4 macrocycles as inhibitors of HCV-NS3 protease. *Bioorg. Med. Chem. Lett.* **2009**, *19*, 2574–2578. (b) Pyun, H.-J.; Chaudhary, K.; Somoza, J. R.; Sheng, X. C.; Kim, C. U. Synthesis and resolution of diethyl(1S,2S)-1-amino-2-vinylcyclopropane-1-phosphonate for HCV NS3 protease inhibitors. *Tetrahedron Lett.* **2009**, *S0*, 3833–3835. (c) Sheng, X. C.; Pyun, H.-J.; Chaudhary, K.; Wang, J.; Doerffler, E.; Fleury, M.; McMurtrie, D.; Chen, X.; Delaney, W. E., IV; Kim, C. U. Discovery of novel phosphonate derivatives as hepatitis C virus NS3 protease inhibitors. *Bioorg. Med. Chem. Lett.* **2009**, *19*, 3453–3457.
- (12) (a) Burk, M. J.; Stammers, T. A.; Straub, J. A. Enantioselective synthesis of α -hydroxy and α -amino phosphonates via catalytic asymmetric hydrogenation. *Org. Lett.* **1999**, *1*, 387–390. (b) Qiu, M.; Hu, X.-P.; Huang, J.-D.; Wang, D.-Y.; Deng, J.; Yu, S.-B.; Duan, Z.-C.; Zheng, Z. Modular phosphine-aminophosphine ligands based on chiral 1,2,3,4-tetrahydro-1-naphthyamine backbone: a new class of practical ligands for enantioselective hydrogenations. *Adv. Synth. Catal.* **2008**, 350, 2683–2689. (c) Zhang, J.; Li, Y.; Wang, Z.; Ding, K. Asymmetric hydrogenation of α and β -enamido phosphonates: rhodium(I)/monodentate phosphoramidite catalyst. *Angew. Chem., Int. Ed.* **2011**, 50, 11743–11747.
- (13) Yan, Z.; Wu, B.; Gao, X.; Chen, M.-W.; Zhou, Y.-G. Enantioselective synthesis of α -amino phosphonates via Pd-catalyzed asymmetric hydrogenation. *Org. Lett.* **2016**, *18*, 692–695.
- (14) Goulioukina, N. S.; Shergold, I. A.; Rybakov, V. B.; Beletskaya, I. P. One-pot two-step synthesis of optically active α -aminophosphonates by palladium-catalyzed hydrogenation/hydrogenolysis of α -hydrazono phosphonates. Adv. Synth. Catal. **2017**, 359, 153–162. (15) (a) Joly, G. D.; Jacobsen, E. N. Thiourea-catalyzed enantioselective hydrophosphonylation of imines: practical access to enantiomerically enriched α -amino phosphonic acids. J. Am. Chem. Soc. 2004, 126, 4102-4103. (b) Saito, B.; Egami, H.; Katsuki, T. Synthesis of an optically active Al(salalen) complex and its application to catalytic hydrophosphonylation of aldehydes and aldimines. J. Am. Chem. Soc. 2007, 129, 1978-1986. (c) Zhang, G.; Hao, G.; Pan, J.; Zhang, J.; Hu, D.; Song, B. Asymmetric synthesis and bioselective activities of α -aminophosphonates based on the dufulin motif. *J. Agric.* Food Chem. 2016, 64, 4207-4213. (d) Li, W.; Wang, Y.; Xu, D. Asymmetric synthesis of α -amino phosphonates by using cinchona alkaloids chiral phase transfer catalyst. Eur. J. Org. Chem. 2018, 2018, 5422-5426.
- (16) Wu, W.; Lin, Z.; Zhu, C.; Chen, P.; Li, J.; Jiang, H. Transition-metal-free [3 + 2] cycloaddition of dehydroaminophosphonates and *N*-tosylhydrazones: access to aminocyclopropanephosphonates with ajacent quaternary tetrasubstituted carbon centers. *J. Org. Chem.* **2017**, *82*, 12746–12756.
- (17) (a) Cheng, X.; Goddard, R.; Buth, G.; List, B. Direct catalytic asymmetric three-component Kabachnik-Fields reaction. *Angew. Chem., Int. Ed.* **2008**, *47*, 5079–5081. (b) Zhou, X.; Shang, D.; Zhang, Q.; Lin, L.; Liu, X.; Feng, X. Enantioselective three-component Kabachnik-Fields reaction catalyzed by chiral scandium-(III)-*N*,*N*′-dioxide complexes. *Org. Lett.* **2009**, *11*, 1401–1404.
- (18) Lefevre, N.; Brayer, J.-L.; Folléas, B.; Darses, S. Chiral α -amino phosphonates via rhodium-catalyzed asymmetric 1,4-addition reactions. *Org. Lett.* **2013**, *15*, 4274–4276.
- (19) Key, H. M.; Miller, S. J. Site- and stereoselective chemical editing of thiostrepton by Rh-catalysed conjugate arylation: new analogues and collateral enantioselective synthesis of amino acids. *J. Am. Chem. Soc.* **2017**, *139*, 15460–15466.
- (20) (a) Trost, B. M.; Ito, H. A direct catalytic enantioselective Aldol reaction via a novel catalyst design. *J. Am. Chem. Soc.* **2000**, *122*, 12003–12004. (b) Trost, B. M.; Ito, H.; Silcoff, E. R. Asymmetric

- Aldol reaction via a dinuclear zinc catalyst: α-hydroxyketones as donors. *J. Am. Chem. Soc.* **2001**, *123*, 3367–3368. (c) Trost, B. M.; Gnanamani, E.; Kalnmals, C. A.; Hung, C.-I. J.; Tracy, J. S. Direct enantio- and diastereoselective vinylogous addition of butenolides to chromones catalyzed by Zn-ProPhenol. *J. Am. Chem. Soc.* **2019**, *141*, 1489–1493. (d) Trost, B. M.; Hung, C.-I. J.; Gnanamani, E. Tuning the reactivity of ketones through unsaturation: Construction of cyclic and acyclic quaternary stereocenters via Zn-ProPhenol catalyzed Mannich reaction. *ACS Catal.* **2019**, *9*, 1549–1557.
- (21) Zhao, D.; Wang, Y.; Mao, L.; Wang, R. Highly enantioselective conjugated addition of phosphite to α,β -unsaturated N-acylpyrroles and imines: a practical approach to enantiomerically enriched amino phosphate. Chem. Eur. J. 2009, 15, 10983–10987.
- (22) Reeves, J. T.; Tan, Z.; Han, Z. S.; Li, G.; Zhang, Y.; Xu, Y.; Reeves, D. C.; Gonnella, N. C.; Ma, S.; Lee, H.; Lu, B. Z.; Senanayake, C. H. Direct titanium-mediated conversion of ketones into enamides with ammonia and acetic anhydride. *Angew. Chem., Int. Ed.* **2012**, *51*, 1400–1404.
- (23) (a) Burk, M. J.; Allen, J. G. A mild amide to carbamate transformation. *J. Org. Chem.* **1997**, *62*, 7054–7057. (b) Faucher, A.-M.; Bailey, M. D.; Beaulieu, P. L.; Brochu, C.; Duceppe, J.-S.; Ferland, J.-M.; Ghiro, E.; Gorys, V.; Halmos, T.; Kawai, S. H.; Poirier, M.; Simoneau, B.; Tsantrizos, Y. S.; Llinàs-Brunet, M. Synthesis of BILN 2061, an HCV NS3 protease inhibitor with proven antiviral effect in humans. *Org. Lett.* **2004**, *6*, 2901–2904.
- (24) Navarre, L.; Martinez, R.; Genet, J.-P.; Darses, S. Access to enantioenriched α -amino esters via rhodium-catalyzed 1,4-addition/enantioselective protonation. *J. Am. Chem. Soc.* **2008**, *130*, 6159–6169.
- (25) Zoń, J. A simple preparation of diethyl 1-acylamino-1-ethenephosphonates. *Synthesis* 1981, 1981, 324.
- (26) Vedejs, E.; Chapman, R. W.; Fields, S. C.; Lin, S.; Schrimpf, M. R. Conversion of arylboronic acids into potassium aryltrifluoroborates: convenient precursors of arylboron difluoride Lewis acids. *J. Org. Chem.* **1995**, *60*, 3020–3027.
- (27) Fernando, J. E. M.; Nakano, Y.; Zhang, C.; Lupton, D. W. Enantioselective N-heterocyclic carbene catalysis that exploits imine umpolung. *Angew. Chem., Int. Ed.* **2019**, *58*, 4007–4011.
- (28) Winter, G.; Lobley, C. M.; Prince, S. M. Decision making in xia2. Acta Crystallogr., Sect. D: Biol. Crystallogr. 2013, 69, 1260–1273.
- (29) Emsley, P.; Lohkamp, B.; Scott, W. G.; Cowtan, K. Features and development of Coot. *Acta Crystallogr., Sect. D: Biol. Crystallogr.* **2010**, *66*, 486–501.
- (30) Murshudov, G. N.; Skubak, P.; Lebedev, A. A.; Pannu, N. S.; Steiner, R. A.; Nicholls, R. A.; Winn, M. D.; Long, F.; Vagin, A. A REFMAC5 for the refinement of macromolecular crystal structures. *Acta Crystallogr., Sect. D: Biol. Crystallogr.* **2011**, *67*, 355–367.
- (31) Freedman, L. D.; Doak, G. O. The preparation and properties of phosphonic acids. *Chem. Rev.* **1957**, *57*, 479–523.